

Copyright  
by  
Deepak Mohan  
2011

**The Thesis Committee for Deepak Mohan  
Certifies that this is the approved version of the following thesis:**

**Synchrophasor Based Methods For Computing the Thevenin  
Equivalent Impedance of A Transmission Network between The  
University of Texas at Austin and The University of Texas PanAm**

**APPROVED BY  
SUPERVISING COMMITTEE:**

**Supervisor:**

---

W. Mack Grady

---

Surya Santoso

**Synchrophasor Based Methods For Computing The Thevenin  
Equivalent Impedance of A Transmission Network between the  
University of Texas at Austin and The University of Texas PanAm**

**by**

**Deepak Mohan, B.E.**

**Thesis**

Presented to the Faculty of the Graduate School of

The University of Texas at Austin

in Partial Fulfillment

of the Requirements

for the Degree of

**Master of Science in Engineering**

**The University of Texas at Austin**

**August 2011**

## **Dedication**

I dedicate this thesis to my mother, Rajee and my father, Ravi Mohan for their faith, support and encouragement throughout the years.

## **Acknowledgements**

I would like to firstly thank Dr. Grady for his guidance and encouragement. Without his vision and motivation, this thesis would not have been possible. I would also like to thank my parents and my friends Yashesh, Nikhil, Pooja, Akanksha, Suyog, Gouri, Lakshmi, Sameer and Jasjyot for their unwavering support and encouragement.

## **Abstract**

### **Synchrophasor Based Methods for Computing The Thevenin Equivalent Impedance of The Transmission Network between The University of Texas at Austin and The University of Texas PanAm**

Deepak Mohan, MSE

The University of Texas at Austin, 2011

Supervisor: W. Mack Grady

With the increase in complexity of modern electricity grids, the implementation of state-estimators has become a vital aspect of stability and contingency analyses for stable and secure power system operation. Transmission line reactance is an important component in the computation of state-estimators. Two models utilizing real-time synchrophasor data and ERCOT load information are proposed to compute Thevenin equivalent reactance. This thesis presents the results of implementing these methods to estimate the equivalent reactance of a transmission network between The University of Texas at Austin and The University of Texas, PanAm.

## Table of Contents

List of Tables .....	ix
List of Figures .....	x
Chapter 1 Introduction .....	1
Chapter 2 Synchrophasors and the Texas Synchrophasor Network .....	3
2.1 Introduction to Synchrophasors .....	3
2.2 The Texas Synchrophasor Network.....	5
2.3 Synchrophasor Applications .....	6
Chapter3 Development of methods to determine Thevenin Equivalent Reactance 7	
3.1 The phase angle.....	8
3.2 The power flow .....	9
3.2.1 Determination of $P_{load}$ .....	10
3.2.2 Determination of $P_{gen}$ .....	10
3.2.2.1The Damping Frequency( $f_{damp}$ ) and the Damping Ratio( $\zeta$ )	
.....	10
3.3 Solving the Power Flow Equation .....	11
3.3.1 Initial Attempt.....	11
3.3.2 The Damping Ratio Method .....	13
3.3.3 Cyclic Variation in Generation Method.....	16
Chapter 4 Results of Analysis and their Interpretation .....	19
4.1 15 <sup>th</sup> February 2011 .....	19
4.1.1 Damping Ratio Method.....	21
4.1.2 Cyclic Variation Method.....	22
4.2 20 <sup>th</sup> February 2011 .....	23
4.2.1 Damping Ratio Method.....	23
4.2.2 Cyclic Variation Method.....	24
4.3 24 <sup>th</sup> February 2011 .....	24
4.3.1 Damping Ratio Method.....	26

4.3.2 Cyclic Variation Method.....	27
4.4 25 <sup>th</sup> February 2011 .....	28
4.4.1 The Damping Ratio Method .....	29
4.4.2 Cyclic Variation Method.....	30
4.5 4 <sup>th</sup> March 2011 .....	30
4.5.1 Damping Ratio Method.....	31
4.5.2 Cyclic Variation Method.....	31
4.6 30 <sup>th</sup> March 2011 .....	32
4.6.1 Damping Ratio Method.....	33
4.6.2 Cyclic Variation Method.....	34
4.7 2 <sup>nd</sup> April 2011 .....	35
4.7.1 Damping Ratio Method.....	35
4.7.3 Cyclic Variation Method.....	36
4.8 3 <sup>rd</sup> April 2011 .....	38
4.8.1 Damping Ratio Method.....	38
4.8.2 Cyclic Variation Method.....	39
4.9 8 <sup>th</sup> April 2011 .....	40
4.9.1 Damping Ratio Method.....	40
4.9.2 Cyclic Variation Method.....	41
4.10 11 <sup>th</sup> April 2011 .....	43
4.10.1 Damping Ratio Method.....	43
4.10.2 Cyclic Variation Method.....	44
Chapter 5 Conclusion.....	45
References.....	47



## List of Tables

Table 1: 19 Feb-Results by Damping Ratio method.....	15
Table 2:19th Feb-Results by Cyclic Variation Method .....	18
Table 3: 15th Feb Results by Damping Ratio Method .....	21
Table 4: Feb 15th-Results by Cyclic Variation Method .....	22
Table 5: Feb 20th-Results by Damping Ratio Method .....	23
Table 6:Feb 20th-Results by Cyclic Variation Method .....	24
Table 7:Feb24th-Results by Damping Ratio Method .....	27
Table 8:Feb24th-Results by Cyclic Variation Method .....	28
Table 9:Feb25th-Results by Damping Ratio Method .....	29
Table 10:Feb25th-Results by Cyclic Variation Method .....	30
Table 11:Mar4-Results by Damping Ratio Method.....	31
Table 12:4th March-Results by Cyclic Variation Method.....	32
Table 13:30th Mar-Results by Damping Ratio Method .....	34
Table 14:30th Mar-Results by Cyclic Variation Method .....	35
Table 15:2nd Apr-Results by Damping Ratio Method .....	36
Table 16:2nd Apr-Results by Damping Ratio Method .....	37
Table 17:3rd April-Results by Damping Ratio Method .....	38
Table 18:3rd April-Results by Cyclic Variation Method .....	39
Table 19:8th Apr-Results by Damping Ratio Method .....	41
Table 20:8th Apr-Results by Cyclic Variation Method .....	42
Table 21:11 Apr-Results by Damping Ratio Method .....	43
Table 22:11th Apr-Results by Cyclic Variation Method .....	44

## List of Figures

Figure 1:Synchrophasors .....	4
Figure 2: The Texas Synchrophasor Network .....	5
Figure 5: Power Flow curves for 21st Feb. by Initial Attempt .....	12
Figure 6:Damping Ratio Profile for 19th Feb.....	13
Figure 7: Load Profile curve 19th Feb.....	14
Figure 8:19 Feb- Power Flow by Damping Ratio Method .....	15
Figure 9: Power Flow and Relative Phase Angles between West Texas and UT Austin .....	16
Figure 10:19th Feb-Power Flow by Cyclic Variation Method .....	18
Figure 11: 15th Feb-Damping Ratio Profile .....	20
Figure 12:Feb 15th-Load Profile curve.....	20
Figure 13:Feb 15th-Power Flow by Damping Ratio Method .....	21
Figure 14: 15th Feb-Power Flow by Cyclic Variation Method .....	22
Figure 15:Feb 20th-Power Flow by Damping Ratio Method .....	23
Figure 16:Feb 20th-Power Flow by Cyclic Variation Method .....	24
Figure 17:24th Feb-Damping Ratio Profile .....	25
Figure 18:Feb 24th Load Profile.....	26
Figure 19:Feb24th-Power Flow by Damping Ratio Method .....	27
Figure 20:Feb24th-Power Flow by Cyclic Variation Method .....	28
Figure 21:Feb25th-Power Flow by Damping Ratio Method .....	29
Figure 22:Feb25th-Power Flow by Cyclic Variation Method .....	30
Figure 23:4thMar-Power Flow by Damping Ratio Method .....	31
Figure 24:4th Mar-Power Flow by Cyclic Variation Method .....	32

Figure 25:30th Mar-Damping Ratio Profile .....	33
Figure 26:30th Mar-Power Flow by Damping Ratio Method .....	34
Figure 27:30th Mar-Power Flow by Cyclic Variation Method .....	34
Figure 28:2nd Apr-Power Flow by Damping Ratio Method .....	36
Figure 29:2nd Apr-Power Flow by Damping Ratio Method .....	37
Figure 30:3rd April-Power Flow by Damping Ratio Method .....	38
Figure 31:3rd April-Results by Cyclic Variation Method .....	39
Figure 32: 8th Apr-Damping Ratio Profile .....	40
Figure 33:8th Apr-Power Flow by Damping Ratio Method .....	41
Figure 34:8th Apr-Power Flow by Cyclic Variation Method .....	42
Figure 35:10 Apr-Power Flow by Damping Ratio Method .....	43
Figure 36:11th Apr-Power Flow by Cyclic Variation Method .....	44

# **CHAPTER 1**

## **INTRODUCTION**

Large scale power systems are extremely complex and have been designed and operated conservatively over years. However, at the present time power systems throughout the world are undergoing fundamental operational changes. Modern power system computer applications have to solve challenges such as congestion, atypical power flow and multiple contingencies [1]. A key challenge is to have a real-time model so that power network computations are performed on a model which resembles the current situation i.e. provides up to date information about the topology from which measurements are derived, and accurate parameters and elements of the model.

An Energy Management system provides a variety of computer applications for the monitoring and control of the power network. State-estimators are one such on-line application which has become vital for the implementation of locational pricing algorithms and stability and contingency analyses. Such analyses are based on a detailed electrical model of the power system which is a simulated model of the real power system that is prepared by each utility's system planners and network engineer specialists by translating the real world equipment and connections of a power system into a mathematical model of the power network that is suitable for solution by computer algorithms [2]. This network model contains the connection information and the electrical characteristics of the equipment such as the reactance of transmission lines. The starting point of most modern power system application thus starts with the estimation of transmission line reactance.

In this thesis, two methods to calculate the Thevenin equivalent reactance of a transmission line are proposed and the results obtained by implementing these methods to calculate the equivalent Thevenin line reactance between The University of Texas at Austin and University of Texas PanAm are presented. The methods utilize real-time synchrophasor data from the grid and load information from the ERCOT website.

Chapter 2 contains a brief introduction to synchrophasors and the Texas Synchrophasor Network.

The basis for formulation of the models is explained in Chapter 3 while Chapter 4 deals with the results and observations of applying the proposed models to compute the equivalent line reactance. The conclusions derived from the analyses are presented in Chapter 5.

## **CHAPTER 2**

### **SYNCHROPHASORS AND THE TEXAS SYNCHROPHASOR NETWORK**

#### **2.1 INTRODUCTION TO SYNCHROPHASORS**

The concept of using synchrophasors to describe power system operating quantities dates back to 1893 when Charles Proteus Steinmetz wrote his paper on mathematical techniques for analyzing AC networks. Although phasors have been clearly understood for over 100 years, the detailed description of a time-synchronized phasor has only recently been codified in the IEEE 1344 “Synchrophasors for Power Systems” standards [3]. Synchronized phasor measurements (synchrophasors) provide real-time measurement of electrical quantities from across a power system. Applications of synchrophasor measurements include system model validation, determining stability margins, maximizing stable system loading, islanding detection, system-wide disturbance recording, and visualization of dynamic system response. The basic system building blocks are GPS satellite-synchronized clocks, phasor measurement units (PMUs), a phasor data concentrator (PDC), and visualization software.

An AC waveform can be mathematically represented by the equation:

$$a(t) = A_m \sin(\omega t + \phi) \quad (1)$$

Where  $A_m$  = magnitude of sinusoidal waveform

$$\omega = 2\pi f$$

$\phi$  = angular starting point of waveform

Note that the synchrophasor is referenced to the cosine function. In a phasor notation, this waveform is typically represented as:

$$\bar{A} = A_m \angle \phi$$

Since in the synchrophasor definition, correlation with the RMS quantity is desired, a scale factor of  $1/\sqrt{2}$  must be applied to the magnitude which results in the phasor representation as:

$$\bar{A} = \frac{A_m}{\sqrt{2}} \angle \phi$$

Adding in the absolute time mark, a synchrophasor is defined as the magnitude and angle of a cosine signal as referenced to an absolute point in time as shown in Figure 1 below.

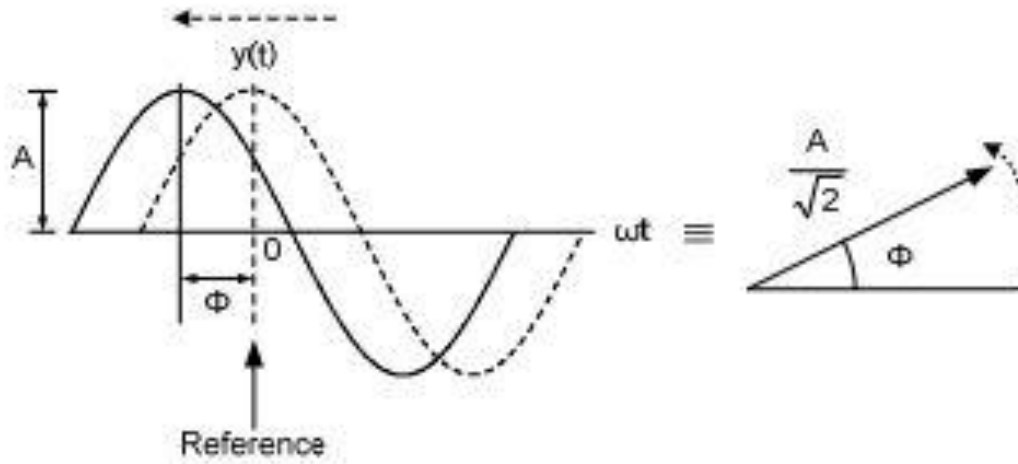


Figure 1: Synchrophasors

A reference sinusoidal signal generated by a GPS clock is identical at every location. The actual voltages and phase angles at point of measurement are compared to reference sinusoidal signal to obtain the phasors. As the measurements are time-stamped by the same GPS clock, comparison can be done on a system wide basis

## 2.2 THE TEXAS SYNCHROPHASOR NETWORK

The state of Texas currently leads the United States with the most installed wind generation capacity. Even though, wind generation is calculated at 8.7% of total installed generation capacity as dependable at peak, wind generation has exceeded 20% of total generation on several days. The Texas synchrophasor network was installed to understand the effect of wind penetration on grid stability and to make informed control decision utilizing real-time grid information[4].

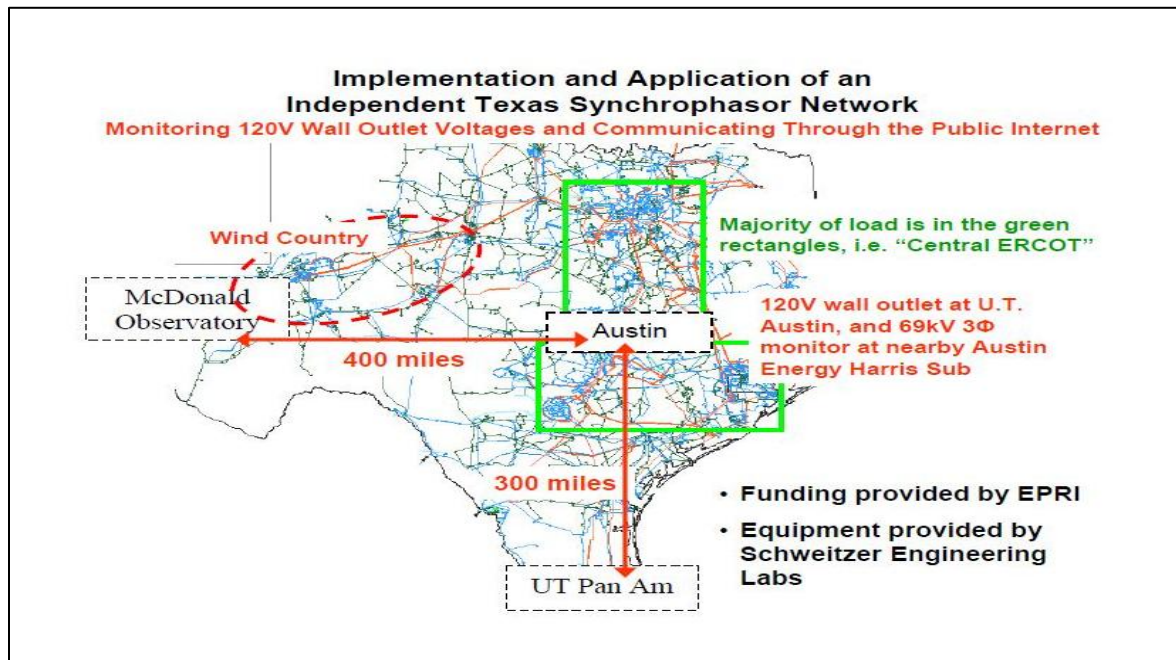


Figure 2: The Texas Synchrophasor Network



Data is being collected at The University of Texas at Austin from PMUs (Phasor Measurement Units) remotely located within the ERCOT grid at McDonald Observatory in West Texas, Schweitzer Engineering Laboratories (SEL), Inc. office at Houston, SEL office at Dallas, SEL office at Boerne near San Antonio, UT Tyler and UT Pan Am. The location of these PMUs within the ERCOT grid is as seen in Figure.2 above. Outside the ERCOT grid PMU data from Western Electricity Coordinating Council (WECC) grid and the Eastern Interconnection are also available. For the methods proposed, data from the Phasor Measurement Unit at the University of Texas PanAm in the Rio Grande Valley was utilized.

## **2.3 SYNCHROPHASOR APPLICATIONS**

Utilities worldwide are deploying synchrophasor systems to monitor and analyze power system behavior. Monitoring and post-event analysis are however only the initial applications of synchrophasors.

With new advances in processing and equipment, synchrophasors are now used to solve a variety of power system protection, automation, and control problems. They are being used to operate and manage the power system. Applications include voltage stability assessment, islanding distributed generation, control based on small signal instability detection, and systemwide disturbance monitoring. Synchrophasor applications By providing a precise, comprehensive view of the entire interconnection, synchrophasors let observers identify changes in grid conditions and help maintain grid stability and security

## CHAPTER 3

### DEVELOPMENT OF METHODS TO DETERMINE THEVENIN EQUIVALENT REACTANCE

The power flow across a transmission line is proportional to the phase angle difference between the sending and the receiving ends. We assume transmission lines and other components such as generators and transformers to be purely inductive, as they have very negligible resistances. The equivalent model of a two bus system can then be represented as shown in the figure below.

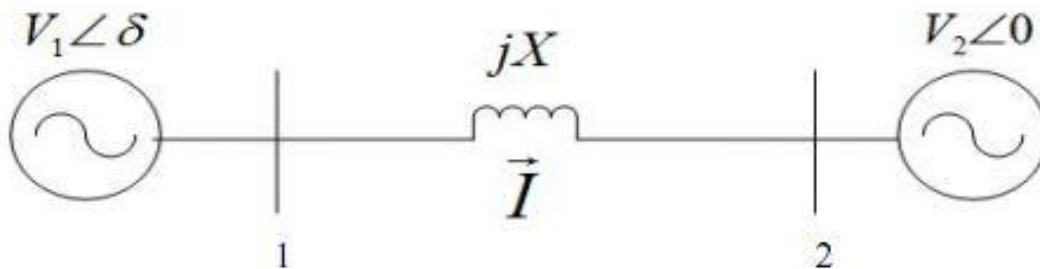


Figure 3: Two bus power system network

The real power transferred between bus 1 and bus 2 depends on the voltage magnitude at each bus, the relative phase angle difference between the buses and the Thevenin equivalent reactance of the entire transmission network between the two buses. It can be mathematically represented as

$$P_{transferred} = \frac{V_1 * V_2}{X_{th\_pu}} \sin(\delta) \quad (2)$$

Where  $V_1$  and  $V_2$  are the voltages at Bus 1 and Bus 2 respectively, ' $\delta$ ' is the relative phase angle between Bus 1 and Bus 2 and  $X_{th}$  is the Thevenin equivalent reactance between Bus 1 and Bus 2. If we represent the entire system in per-unit terms, the equation 2 above is modified as

$$P_{transferred}(pu) = \frac{1*1}{X_{th\_pu}} \sin(\delta) \quad (3)$$

Equation 3 must be solved to obtain the per-unit value of the Thevenin equivalent reactance  $X_{th\_pu}$ . In order to estimate the Thevenin Equivalent reactance, the data received from the remote PMU locations is archived and analyzed using SEL programs such as the SVP Configurator, SEL-5078 SynchroWAVE Console and the SEL-5076 SynchroWAVE Archiver. This data is used to estimate the power flow in the transmission line and the relative phase angle between the two buses. The procedure to obtain the data is explained in the next few sections

### 3.1 THE PHASE ANGLE

As seen in Equation 3 the real power flow across the two-bus transmission network is directly proportional to the sine of the relative phase angle difference between the two buses.

The Visual Basic program 'PMU\_Daily\_Screener' written at The University of Texas at Austin is used to obtain the relative phase angle  $\delta$  between the University of Texas at Austin and The University of Texas PanAm. The output of the program consists of two time-stamped CSV files for each hour of the day under consideration. One of the CSV files contains hourly reports detailing drop-outs or errors in data, voltage magnitudes at the sending and receiving end PMU's and frequency deviations in that

time interval. The other CSV file contains average phase angle magnitudes for each minute of the hour under consideration.

We consider the output file which has the phase angle averages. The program is run specifically for UT PanAm and hourly phase angle average is computed which is used in the calculations to determine the Thevenin equivalent reactance for a particular day.

### 3.2 THE POWER FLOW

Once we obtain the phase angle, we determine the power flow across the transmission line. We assume that there is a net import of power into the Rio-Grande valley, ie most of the generation  $P_{gen}$  is concentrated around Bus 3 which represents Central ERCOT region which is feeding the load connected to Bus 5 which represents the Rio Grande Valley. The proposed system is as shown in the figure below and it is assumed that it is sufficient to determine the Thevenin equivalent reactance.

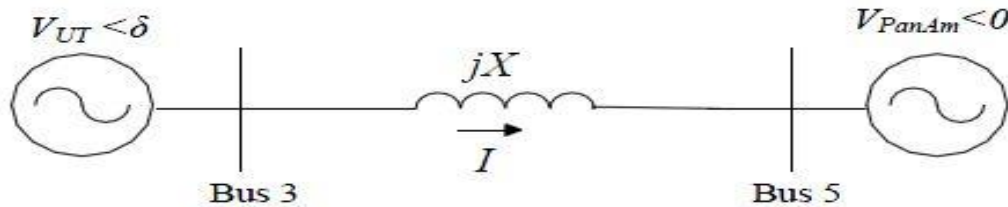


Figure 4: Proposed two bus system

The net power flow in the proposed two-bus system represented in Figure is thus given by equation (4) below

$$P_{transferred} = P_{gen} - P_{load} \quad (4)$$

Once the power flow is computed and with phase angle  $\delta$  already known, Equation 3 can be solved for a particular day to obtain the Thevenin equivalent reactance  $X_{th}$ .

### **3.2.1 Determination of $P_{load}$**

The first step in computing the power flow is to procure the load information for the southern part of the ERCOT grid where the University of Texas PanAm is located. This is obtained from the ERCOT website under the Grid Information section at [http://www.ercot.com/content/cdr/html/20110522\\_actual\\_loads\\_of\\_weather\\_zones](http://www.ercot.com/content/cdr/html/20110522_actual_loads_of_weather_zones)

The link is updated on an hourly basis with information about the load drawn at various regions in the ERCOT grid. We assume that the load drawn the Southern ERCOT region represents the net load connected to Bus 5 (the Rio Grande valley) in our simplified two bus system depicted in Figure 4.

### **3.2.2 Determination of $P_{gen}$**

Generation data is not as readily available as load data and hence we have to devise methods to represent the generation  $P_{gen}$  as a function of known phasor quantities. Knowing the close relationship between generation and easily measurable phasor data such as the grid damping-ratio ( $\zeta$ ) and the damping frequency ( $f_{damp}$ ), we try to find a correlation between generation and these quantities.

#### **3.2.2.1 The Damping Frequency ( $f_{damp}$ ) and the Damping Ratio ( $\zeta$ )**

The Visual Basic program ‘PMU\_Modal\_Analysis’ written at the University of Texas at Austin by Dr. Grady is used to determine the damping frequency and the damping ratio. The output of the program consists of three plots, a scatter plot of modal frequencies and damping ratios, time trend of modal frequencies and magnitudes and a

time trend of modal frequencies and damping ratios. The scatter plot of modes of the power system as a function of time is pertinent to this thesis. To make interpretation of the scatter plot easier, a text-box is provided at the bottom of the plot which represents the values of the damping frequency, damping ratio and the magnitude of the top ¼ oscillations in the system under consideration in that time interval. For the purpose of this thesis, we record the values of the damping ratio and damping frequency at hourly intervals for the particular day under consideration.

The various methods developed to solve the power flow equation differ from each other in the way  $P_{gen}$  is represented as a function of known quantities and the way these methods were developed is explained in the following sections.

### 3.3 SOLVING THE POWER FLOW EQUATION

We try various methods to solve the power flow equation to obtain the Thevenin Equivalent reactance with the known quantities at our disposal. These methods differ from each other in the way  $P_{gen}$  is represented.

#### 3.3.1 Initial Attempt

We assume that the generation is inversely proportional to the damping frequency. Thus  $P_{gen}$  can be represented as

$$P_{gen} = \frac{A}{f_{damp}}$$

Ignoring transmission losses, the power flow equation can now be represented as

$$\frac{A}{f_{damp}} - P_{load} = \frac{\sin(\delta)}{X_{th\_pu}} \quad (5)$$

where all quantities are converted into per-unit on a 100 MVA base and A is constant for the period being analyzed ie an entire day. Equation 5 can now be solved to obtain  $X_{th\_pu}$ .

We begin by entering the values of known data in an Excel spreadsheet. The Excel Solver is now applied to minimize the sum of the squared errors between the Left Hand Side and Right Hand Side of equation() by varying the values of A and  $X_{th\_pu}$ . In mathematical terms the Excel solver is used to minimize the sum of squared errors given by Equation 6 below.

$$\sum_0^{23} \left[ \frac{A}{f_{damp}} - P_{load} - \frac{\sin(\delta)}{X_{th\_pu}} \right]^2 \quad (6)$$

Where n=0 to 23 represents the hours of the day under consideration.

The results of using this method for data obtained on 19<sup>th</sup> February 2011 are presented in Figure 5 below.

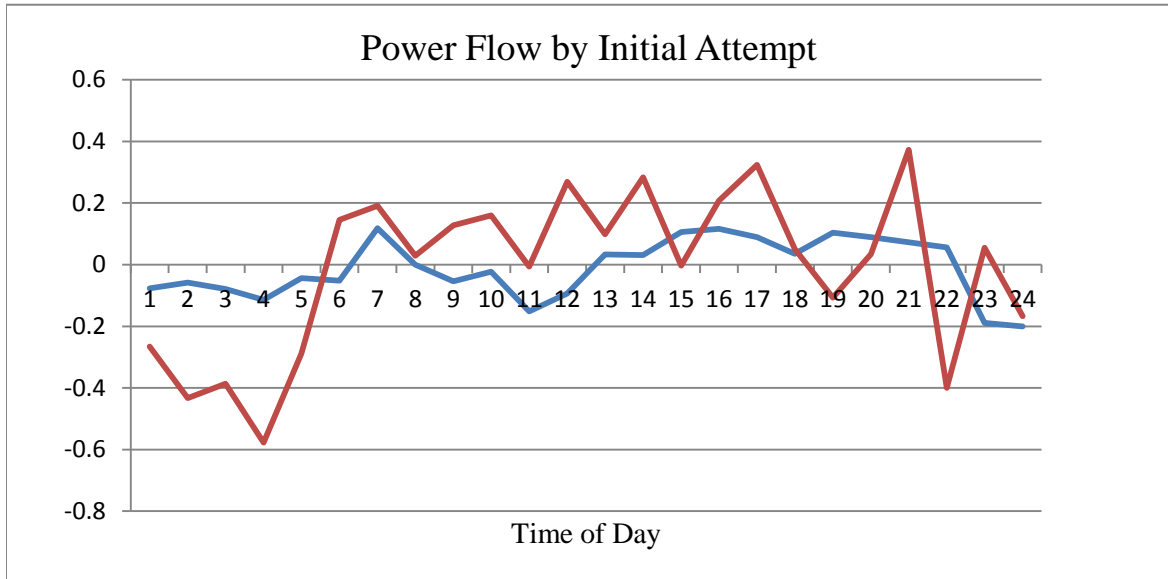


**Figure 5: Power Flow curves for 21st Feb. by Initial Attempt**

As can be seen, the solution fails to converge for  $X_{th\_pu}$  within a realistic range of values and the curves for the L.H.S and R.H.S of the power flow equation fail to fit properly with a large value of error. The analysis was repeated for various days with the similar results and hence this initial method to estimate the power generation  $P_{gen}$  was discarded.

### 3.3.2 The Damping Ratio Method

This method was devised after observing the close fit between the daily load profile and damping ratio curves for synchrophasor data collected over the month of February. As an example the curves for February 19<sup>th</sup> 2011 are presented below.

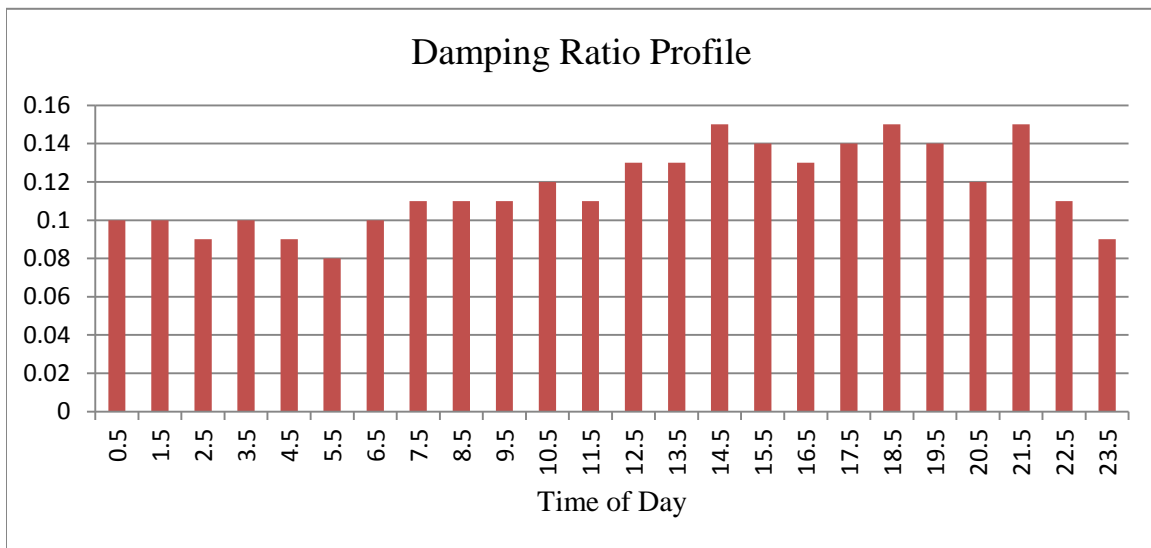


Figure 6:Damping Ratio Profile for 19th Feb.



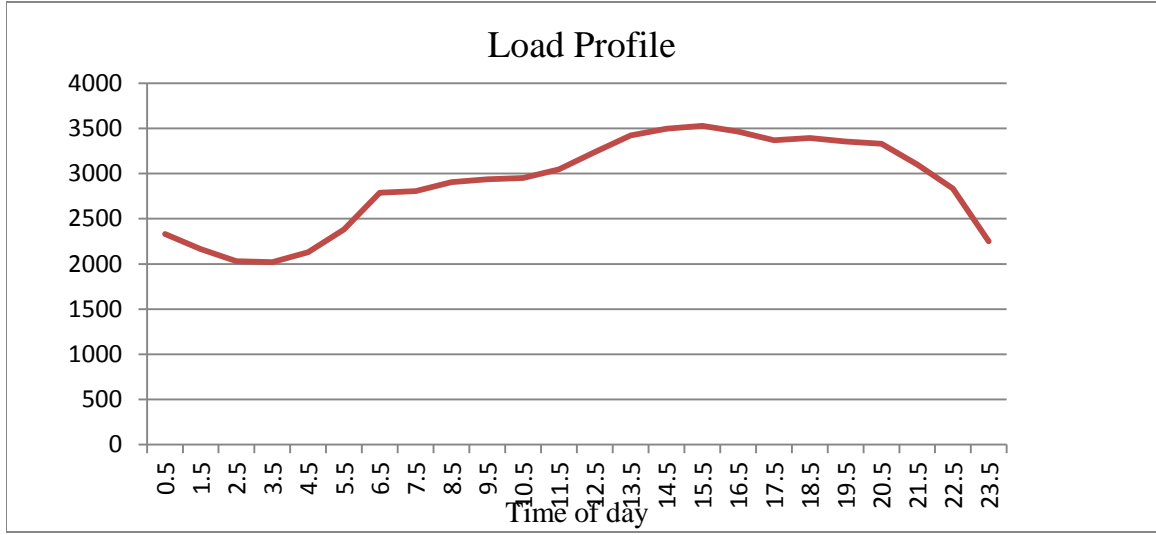


Figure 7: Load Profile curve 19th Feb.

Knowing that the generation profile must closely follow the load profile to ensure that the load requirements are satisfied, we try to find a correlation between  $P_{gen}$  and the damping ratio( $\zeta$ ). Through trial and error, we find that representing  $P_{gen}$  as follows

$$P_{gen} = A * \zeta + B \quad (7)$$

gives us the best results. A and B are constants for the period under consideration which is an entire day. Substituting equation 7 in the power flow equation (), we get

$$A * \zeta + B - P_{load} = \frac{\sin(\delta)}{X_{th\_pu}} \quad (8)$$

where all quantities are expressed on a 100MVA base.

The modified power flow equation represented by Equation 8 above is now solved to estimate  $X_{th\_pu}$ . The known data is entered into an Excel Spreadsheet and the Excel Solver is used to minimize the square of the errors between the L.H.S and R.H.S of

equation 8 by varying the values of A,B and  $X_{th\_pu}$  . Mathematically the Excel Solver can be represented as

$$\sum_{n=0}^{23} [A * \zeta + B - P_{load} - \frac{\sin(\delta)}{X_{th\_pu}}]^2 \quad (9)$$

Where n =0 to 23 represents each hour of the day under consideration.

The results of applying the Excel Solver represented in Equation 9 to the synchrophasor data obtained on February 19<sup>th</sup> 2011 are shown below.

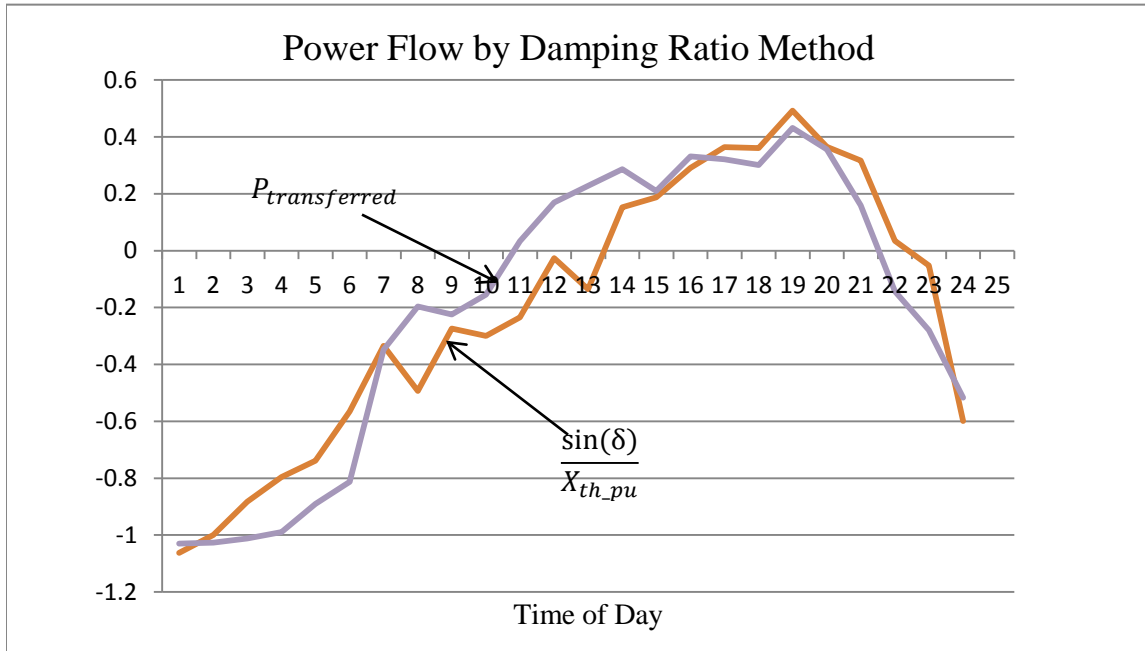


Figure 8:19 Feb- Power Flow by Damping Ratio Method

Day	A	B	$X_{th\_pu}$	Error
19-Feb-2011	1.2E4	1354.78	0.041	0.0279

Table 1: 19 Feb-Results by Damping Ratio method

As can be seen from Figure 8 and Table 1, a realistic estimate of  $X_{th\_pu}$  is obtained and there is a better curve fit between the L.H.S and R.H.S of the power flow equation than obtained by the initial method. The error is also minimized. The result of using this method to analyze data for several days is presented in the next chapter

### 3.3.3 Cyclic Variation in Generation Method

Analysis for several days using the Damping Ratio method gives us a realistic range of values for  $X_{th\_pu}$  and a good curve fit for the power flow with low values of error. However this is not sufficient to conclude the estimated values for  $X_{th\_pu}$  and another method must be devised to corroborate the findings of the Damping Ratio method.

The Cyclic Variation in Generation Method was devised by observing the strong correlation between the graphs for power flow and phase angle difference between West Texas and the Central ERCOT grid as shown in the Figure 9 below.

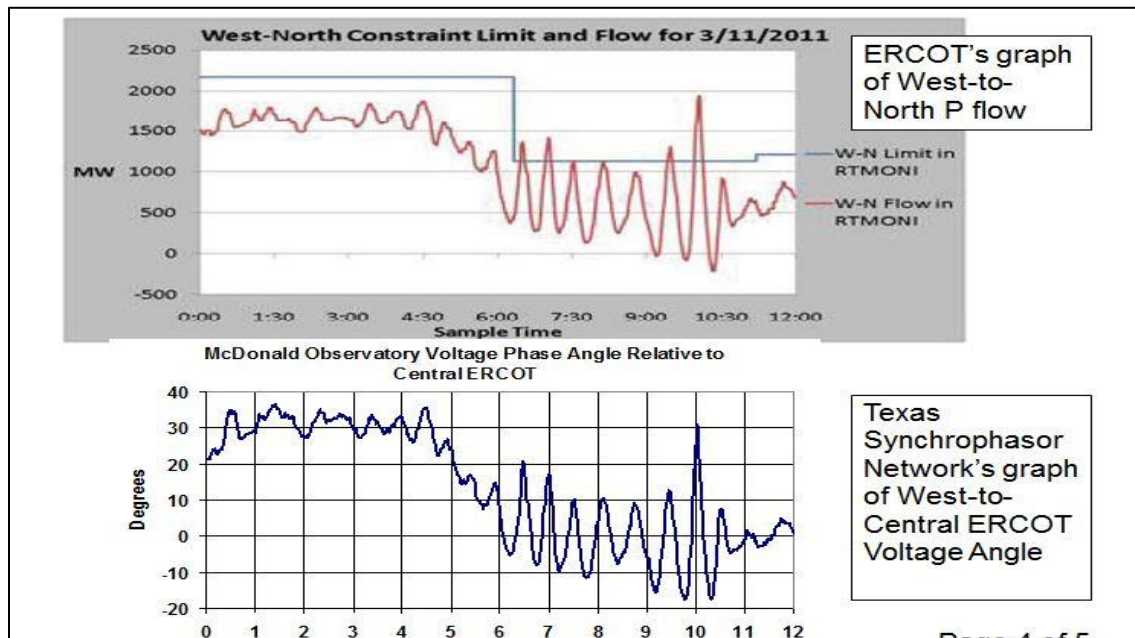


Figure 9: Power Flow and Relative Phase Angles between West Texas and UT Austin

We take advantage of the strong correlation between power flow and phase angle to formulate an expression for  $P_{export}$  which is given by the difference between generation  $P_{gen}$  and  $P_{load}$ . Since  $P_{load}$  is a known quantity, we attempt to express  $P_{gen}$  as a function of the hourly variation in phase angle over the duration of an entire day. The nearly sinusoidal nature of the load profile waveform observed over the duration of several months leads to the following expression for  $P_{gen}$

$$P_{gen} = A * \sin(15 * (H + B)) + C \quad (10)$$

where A,B and C are constants for the period under consideration and H varies from 1 to 24 to simulate the hourly variation in phase angle.

The power flow expression now gets modified as

$$A * \sin(15 * (H + B)) + C - P_{load} = \frac{\sin(\delta)}{X_{th\_pu}} \quad (11)$$

where all quantities are expressed on a 100MVA base.

The modified power flow equation can now be solved to obtain the Thevenin equivalent reactance for a particular day. Using the Excel Solver as before, we try to minimize the sum of the square of the errors between the L.H.S and R.H.S of Equation 11 by varying the values of A,B,C and  $X_{th\_pu}$ . The expression to be minimized can be mathematically represented as

$$\sum_{n=0}^{23} [A * \sin(15 * (H + B)) + C - P_{load} - \frac{\sin(\delta)}{X_{th\_pu}}]^2 \quad (12)$$

The results of applying this method on synchrophasor data for February 19<sup>th</sup> 2011 are shown in Figure 10 below.

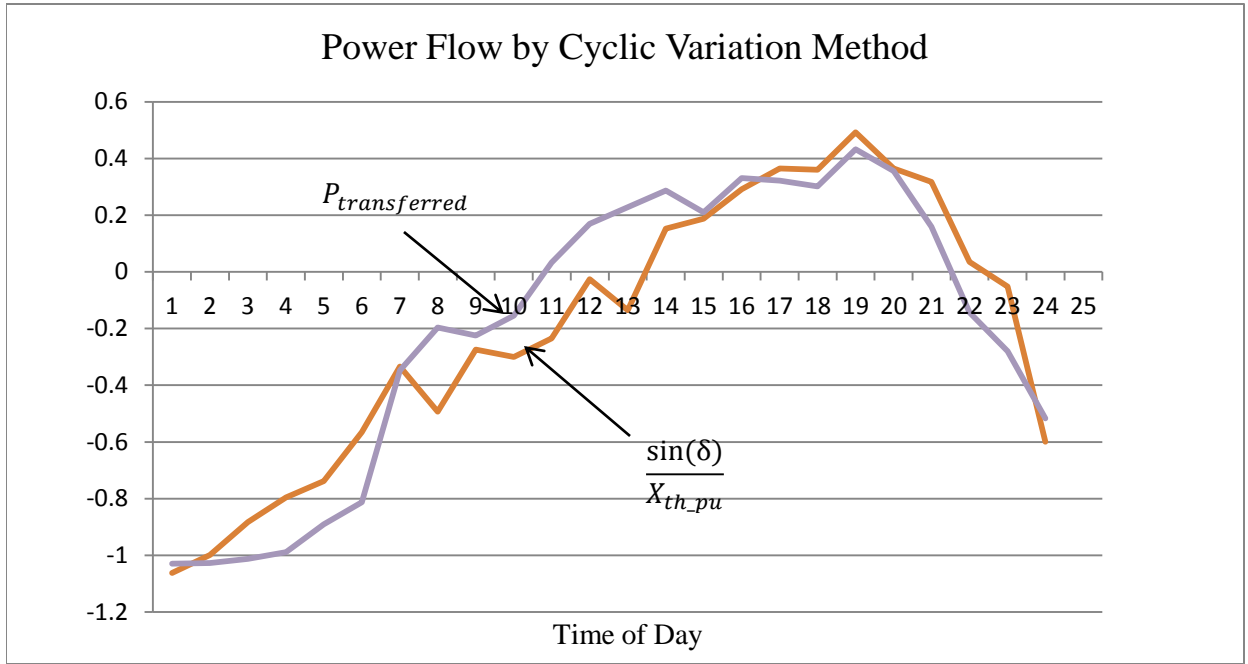


**Figure 10:19th Feb-Power Flow by Cyclic Variation Method**

Day	A	B	C	Xth_pu	Error
19-Feb-2011	579.43	14.1	2900.91	0.049	0.021

**Table 2:19th Feb-Results by Cyclic Variation Method**

As can be seen from Figure 10 and Table 2, we get a realistic prediction of  $X_{th\_pu}$ , a good curve fit between the two estimates for the power flow and a reduced value of error. The estimated value of  $X_{th\_pu}$  is quite close to the estimate obtained by the Damping Ratio Method. We now apply the Cyclic Variation in Generation Method on synchrophasor data for several days. The results of such analysis are presented in the next chapter

## **CHAPTER 4**

### **RESULTS OF ANALYSIS AND THEIR INTERPRETATION**

The synchrophasor data is tagged according to UTC whereas load data on the ERCOT website is according to Central Standard Time (CST). The synchrophasor data therefore requires time correction before it can be used.

The damping ratio and load profile curve show good correlation for most of the days under analysis. Due to the similarity in waveforms for days with good correlation, the waveforms are not presented for such days except for the first day to show the correlation. Grid events can cause anomaly in the damping ratio data and for such days the damping ratio and load profile curve is presented and the impact of grid events on the results of the analysis is discussed. As we have only 24 data points for a particular day, removing the anomalous data points prevents the Excel Solver converging to the required solution and hence anomalous data points are retained while performing the analysis.

The observations and results of analysis for several days are presented in the following sections.

#### **4.1 15<sup>TH</sup> FEBRUARY 2011**

The synchrophasor data obtained for 15<sup>th</sup> February shows a strong correlation between the damping ratio and load profile as shown in Figures 11 and 12 below. We expect to get a good curve-fit for the power flow estimates by the two methods and the results of the analyses are presented in the following sections

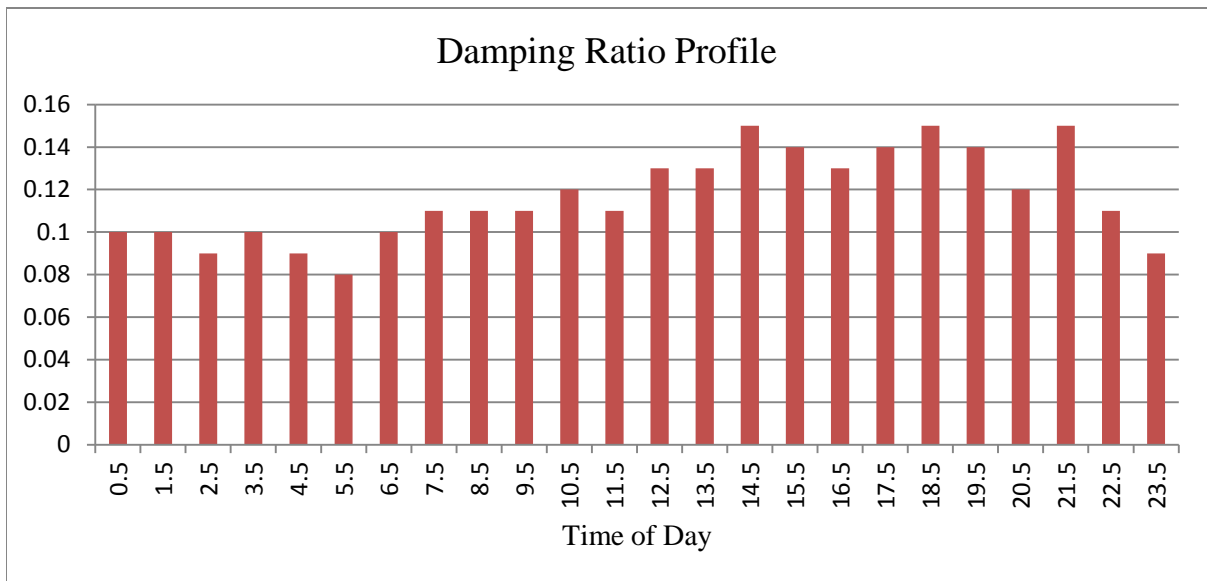


**Figure 11: 15th Feb-Damping Ratio Profile**

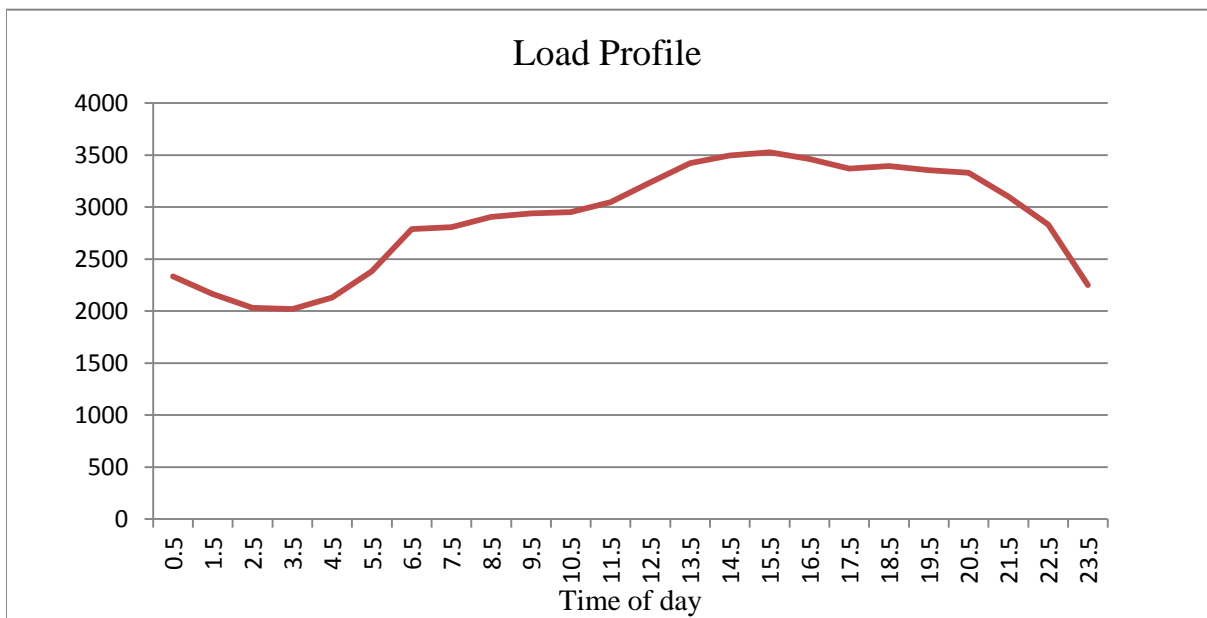


**Figure 12:Feb 15th-Load Profile curve**

#### 4.1.1 Damping Ratio Method

The synchrophasor data obtained on February 15<sup>th</sup> 2011 is entered into an Excel Spreadsheet. The Excel solver is set to minimize the sum of squared errors between the L.H.S and R.H.S of Equation 9 by varying A,B and  $X_{th\_pu}$ . The results of analysis shows a good curve fit between the two estimates of the power flow between the University of Texas at Austin and The University of Texas at PanAm as shown by Figure 13 below. The value of  $X_{th\_pu}$  obtained is consistent with values obtained throughout the months of March and April as seen in the coming sections.

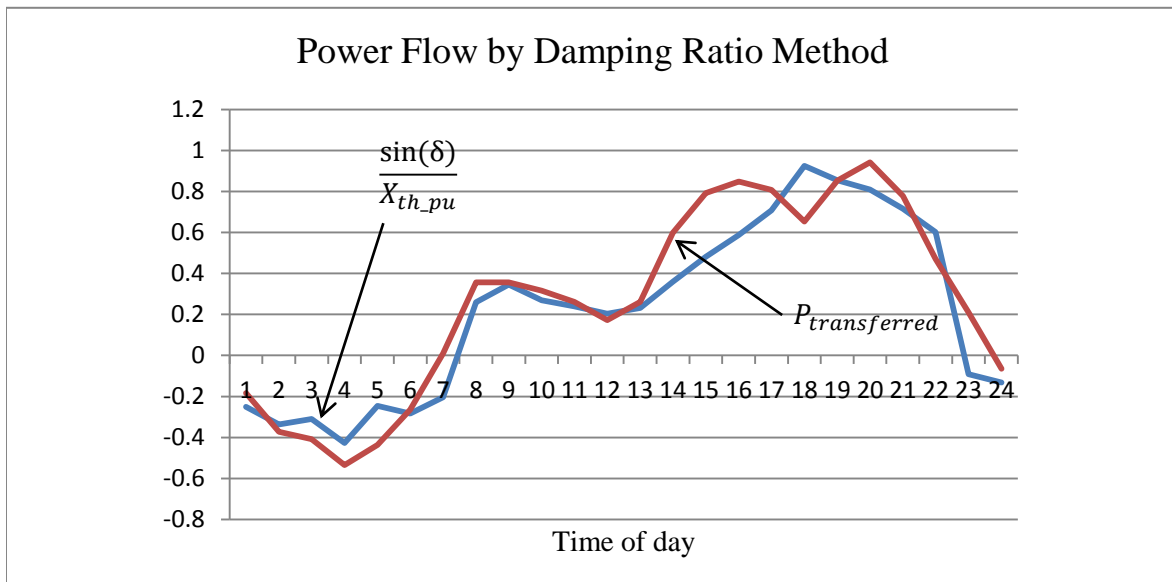


Figure 13:Feb 15th-Power Flow by Damping Ratio Method

Day	A	B	$X_{th\_pu}$	Error
15-Feb-2011	0.7E4	1476.62	0.04	0.07

Table 3: 15th Feb Results by Damping Ratio Method



#### 4.1.2 Cyclic Variation Method

Similar to the Damping Ratio method, the Excel Solver is set to minimize the sum of the squared errors between the L.H.S and R.H.S of Equation 12 by varying A,B,C and  $X_{th\_pu}$ . The results of the analysis are presented below in Figure 14 and Table 4. We get a curve fit between the two power flow estimates and a consistent value for  $X_{th\_pu}$ .

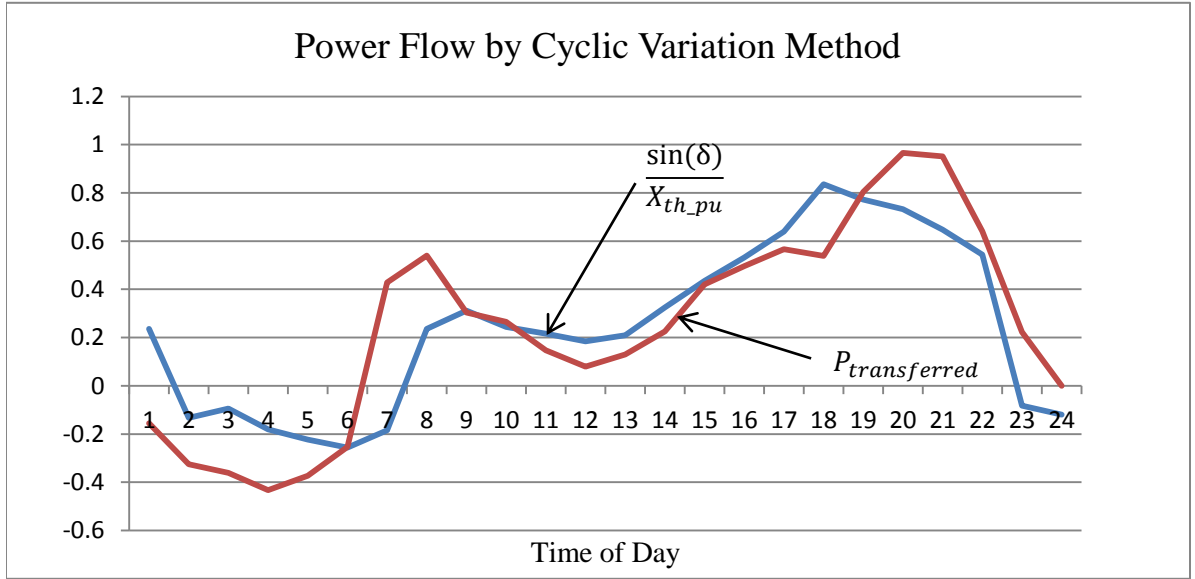


Figure 14: 15th Feb-Power Flow by Cyclic Variation Method

Day	A	B	C	$X_{th\_pu}$	Error
15-Feb-2011	286.29	15.51	2530.61	0.0407	0.0503

Table 4: Feb 15th-Results by Cyclic Variation Method

The power flow curve estimates obtained by both methods are similar and we get similar values for  $X_{th\_pu}$ . The same steps were used to analyze the synchrophasor data for the remaining days and the results are presented in the following sections.

## 4.2 20<sup>TH</sup> FEBRUARY 2011

Following the same steps for analysis as in the case of 15<sup>th</sup> February 2011, the synchrophasor data obtained for 20<sup>th</sup> February is analyzed using both methods. The results are presented in the sections below.

### 4.2.1 Damping Ratio Method

The Damping Ratio method gives a good curve fit for both estimates of the power flow and the value of  $X_{th\_pu}$  is very similar to that obtained for 15<sup>th</sup> February with a very small value of error. The results of analysis are presented in Figure 15 and Table 5 below.

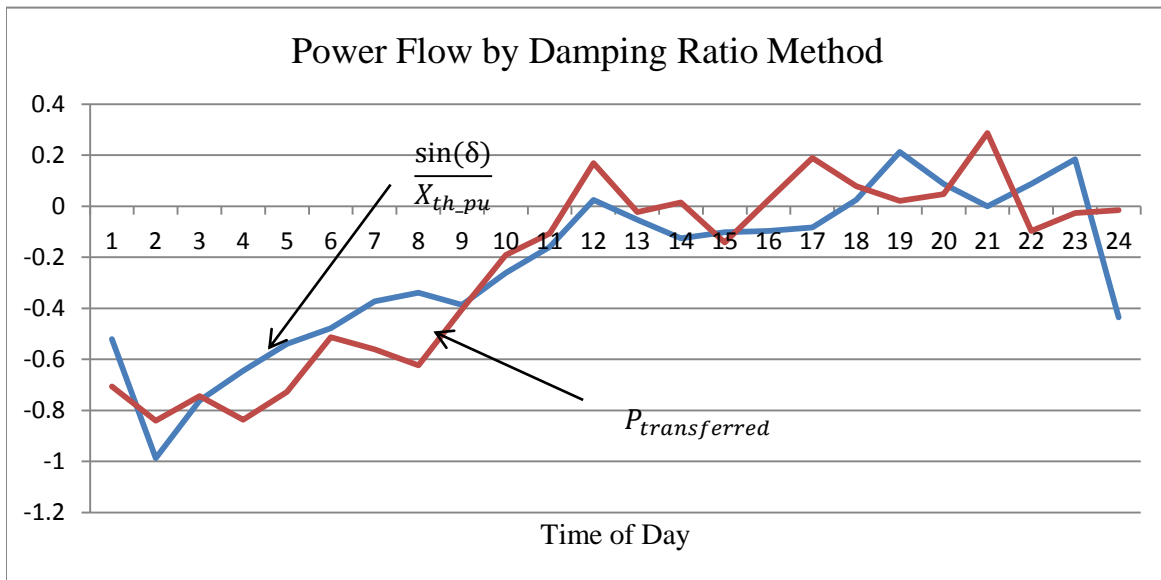


Figure 15:Feb 20th-Power Flow by Damping Ratio Method

Day	A	B	$X_{th\_pu}$	Error
20-Feb-2011	1.0E4	1521.67	0.035	0.025

Table 5: Feb 20th-Results by Damping Ratio Method

#### 4.2.2 Cyclic Variation Method

The results obtained by the Cyclic variation method correspond to those obtained by the Damping Ratio method and are presented in Figure 16 and Table 6 below.

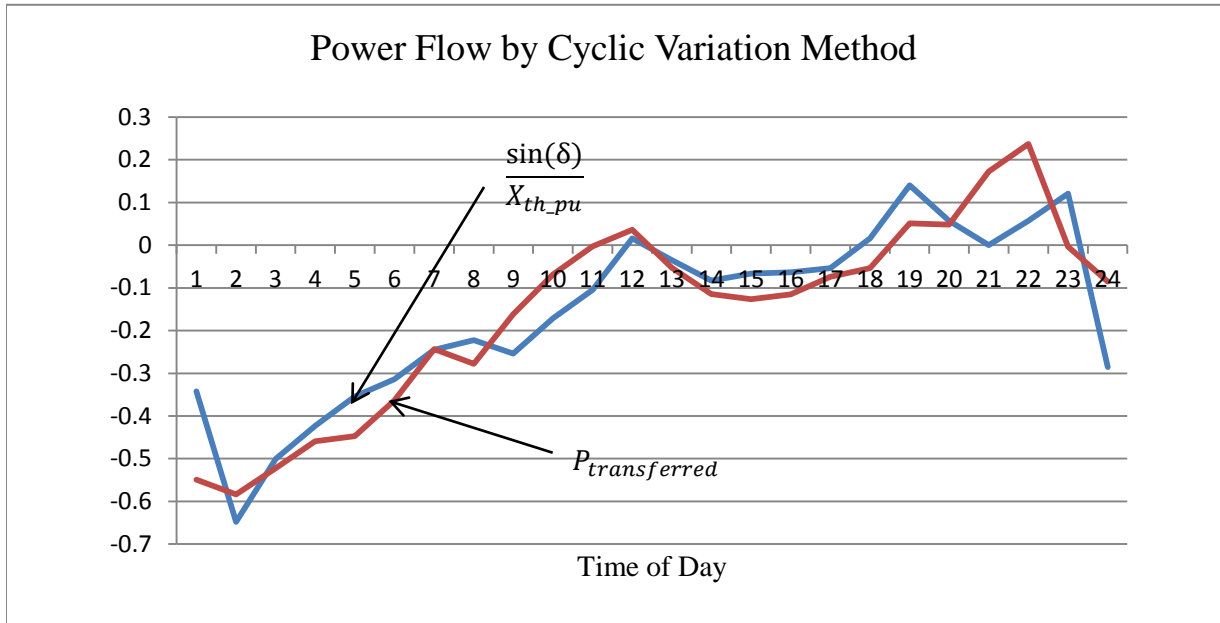


**Figure 16:Feb 20th-Power Flow by Cyclic Variation Method**

Day	A	B	C	$X_{th\_pu}$	Error
20-Feb 2011	491.24	13.11	2719.03	0.044	0.0009

**Table 6:Feb 20th-Results by Cyclic Variation Method**

We see that a good curve fit is obtained for all intervals of the day and the waveforms obtained match closely with the results of the Damping Ratio Method.

#### 4.3 24<sup>TH</sup> FEBRUARY 2011

The synchrophasor data obtained on 24<sup>th</sup> February 2011 shows a spike in the damping ratio curve for the day at CST 19:00 and 20:00 as shown in Figure 17 below due

to an unknown grid event. It can be seen from the load profile curve shown in Figure 18 that there is a deviation between the load profile and damping ratio curve. This deviation may cause variation in the Thevenin equivalent reactance obtained at the end of the analysis.

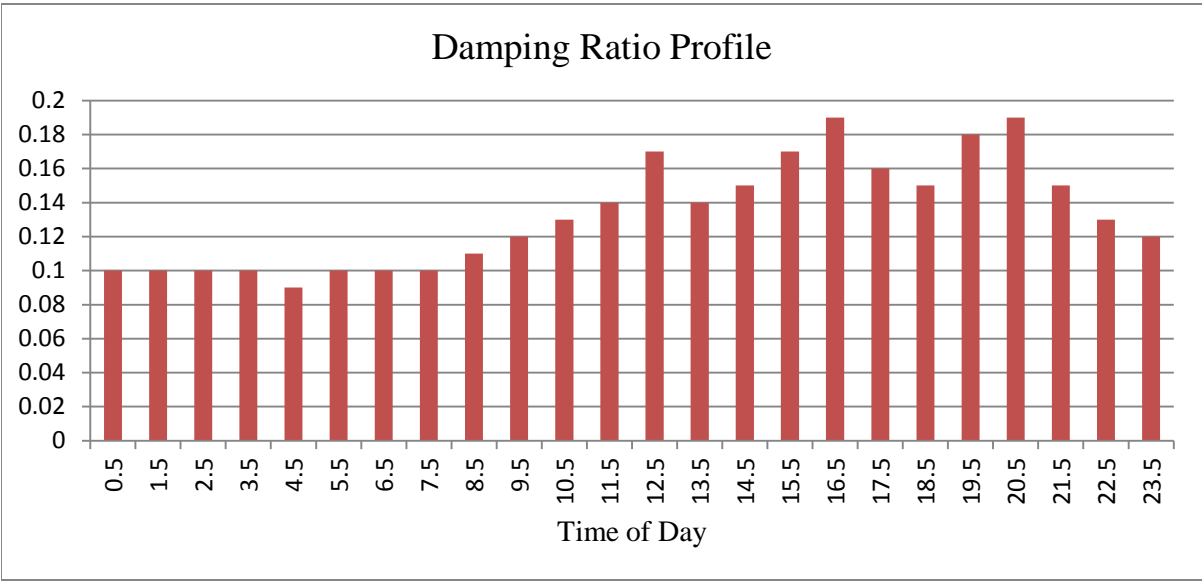


**Figure 17:24th Feb-Damping Ratio Profile**

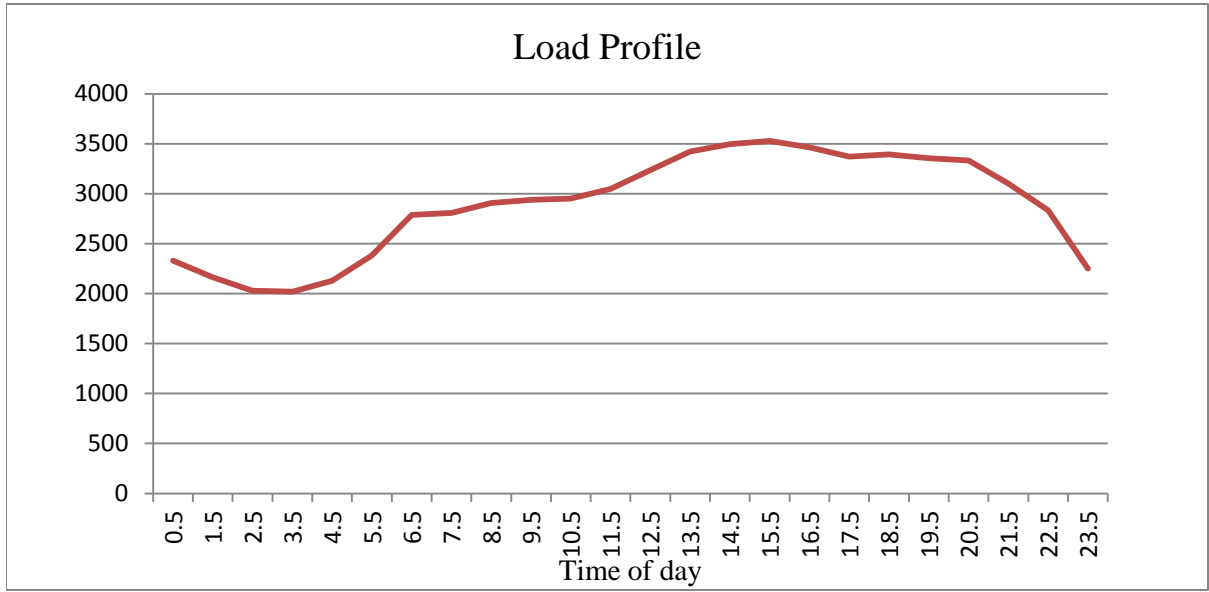
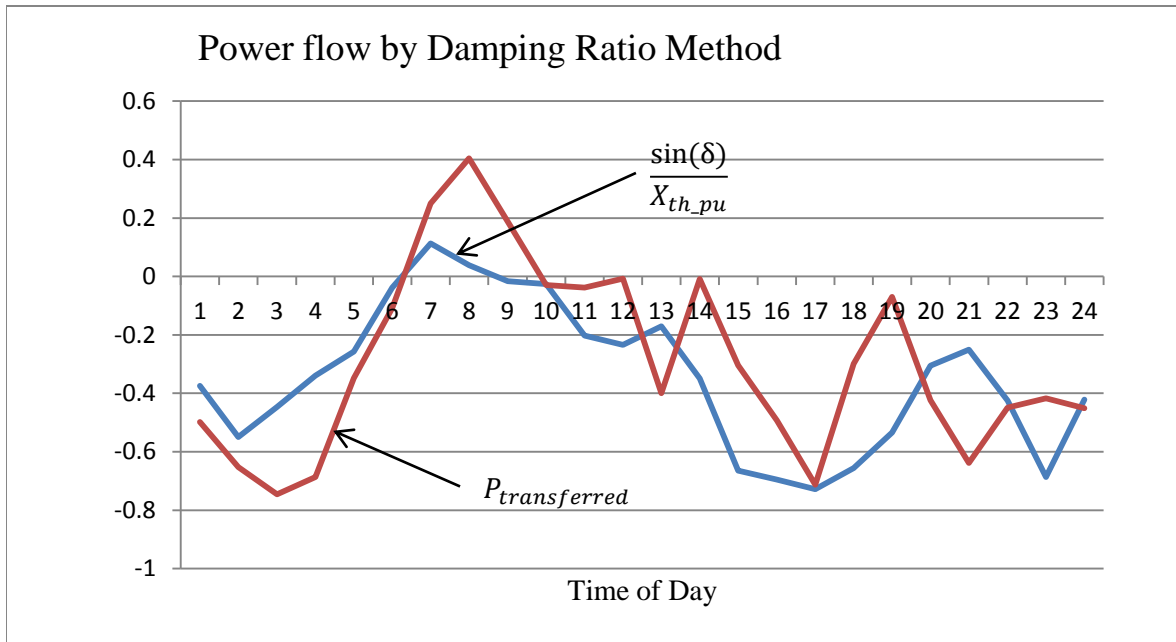


Figure 18:Feb 24th Load Profile

#### 4.3.1 Damping Ratio Method

The synchrophasor data obtained is analyzed using the Damping Ratio method. As expected we do not get a good curve fit between the two estimated power flow curves. This is because we express  $P_{gen}$  as a function of damping ratio ( $\zeta$ ) and the anomaly in the damping ratio data affects the correlation between the generation and load. The anomalous data points cannot be eliminated as we have only 24 data points for each day and removing them results in a non-convergence of the Excel Solver solution. The results of the analysis are presented in Figure 19 and Table 8 below.



**Figure 19:Feb24th-Power Flow by Damping Ratio Method**

Day	A	B	$X_{th\_pu}$	Error
24-Feb-2011	1.3E4	1319.44	0.04	0.06

**Table 7:Feb24th-Results by Damping Ratio Method**

#### 4.3.2 Cyclic Variation Method

Using the same steps, the synchrophasor data is analyzed using the Cyclic Variation method. As seen in Figure 20, the power flow curves obtained show a better curve fit as opposed to the Damping Ratio method.

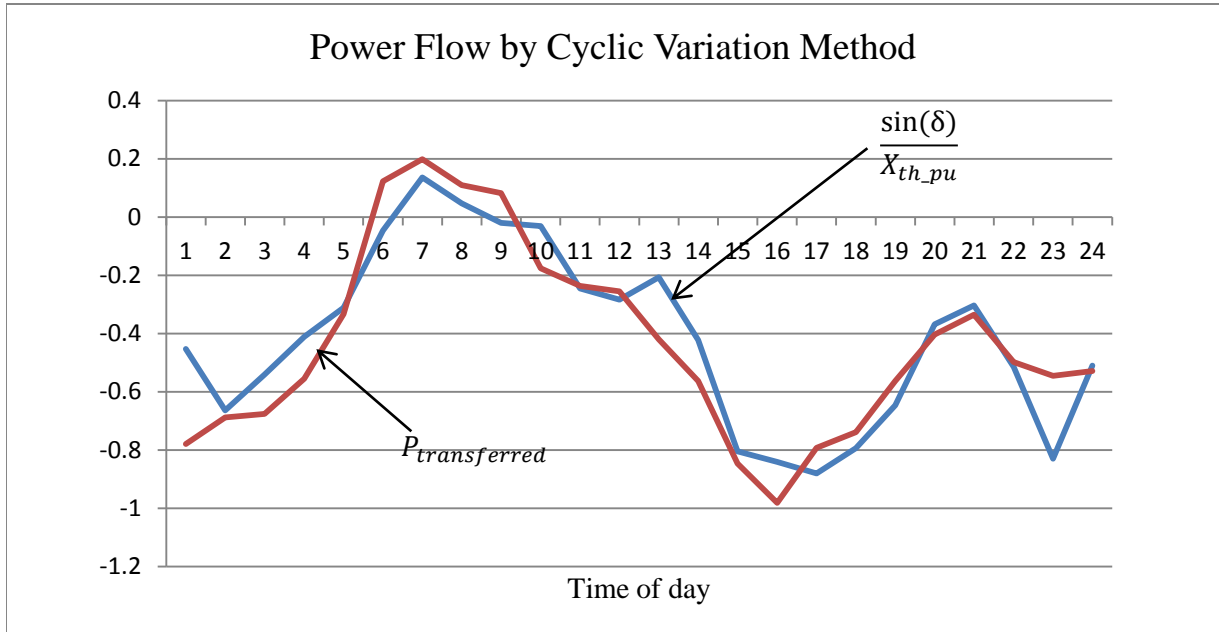


**Figure 20:Feb24th-Power Flow by Cyclic Variation Method**

Day	A	B	C	$X_{th\_pu}$	Error
24-Feb-2011	704.28	13.19	3189.29	0.0444	0.016

**Table 8:Feb24th-Results by Cyclic Variation Method**

We however see that the value of the Thevenin equivalent reactance is not affected by the anomaly in damping ratio data and the value obtained is consistent for the values seen for the rest of the month of February. With the availability of grid information reports, a correlation between grid events and the corresponding effect on grid parameters can be made.

#### 4.4 25<sup>TH</sup> FEBRUARY 2011

The sychrophasor data obtained is analyzed using both methods. Unlike the previous day, there is no anomaly in the damping ratio data and hence we expect a good

fit in the power flow curves using both methods. The results of the analysis are presented in the following sections.

#### 4.4.1 The Damping Ratio Method

Analysis by the damping ratio method gives a good curve fit between the two estimates for the power flow curve as shown in Figure 21 below. The Thevenin equivalent reactance obtained by the analysis is consistent with past results.

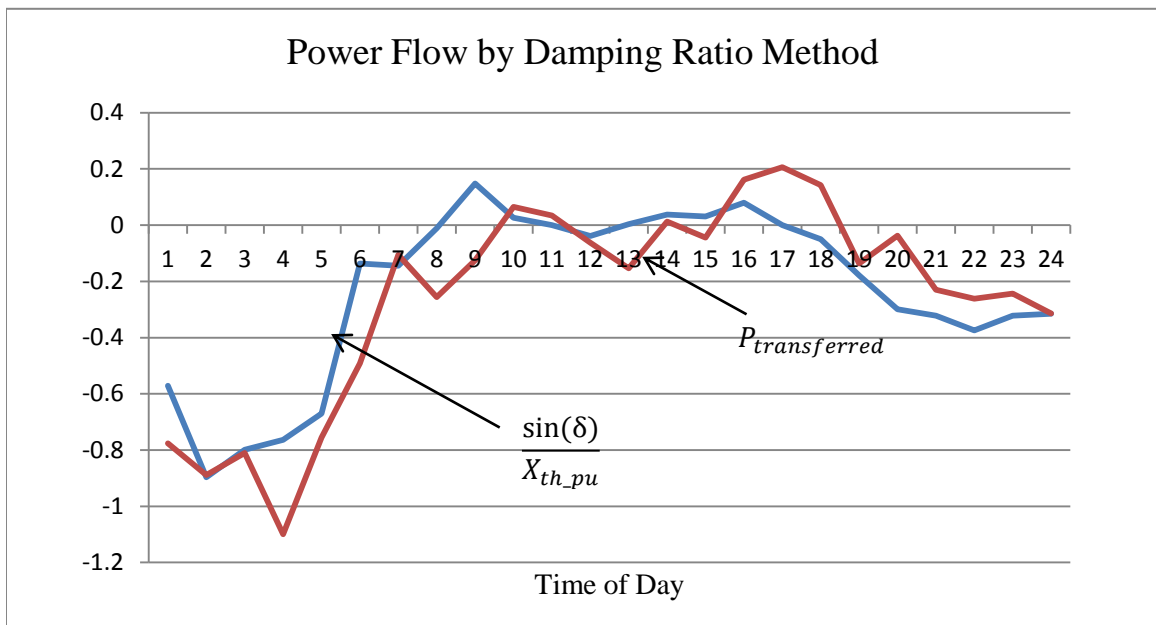


Figure 21:Feb25th-Power Flow by Damping Ratio Method

Day	A	B	$X_{th\_pu}$	Error
25-Feb-2011	1.3E4	1000	0.045	0.027

Table 9:Feb25th-Results by Damping Ratio Method



#### 4.4.2 Cyclic Variation Method

Analysis by the Cyclic Variation method gives good curve fit as shown in Figure 22 below and the Thevenin equivalent reactance values is similar to value obtained by the Damping Ratio method and similar power flow curves are obtained with a low error.

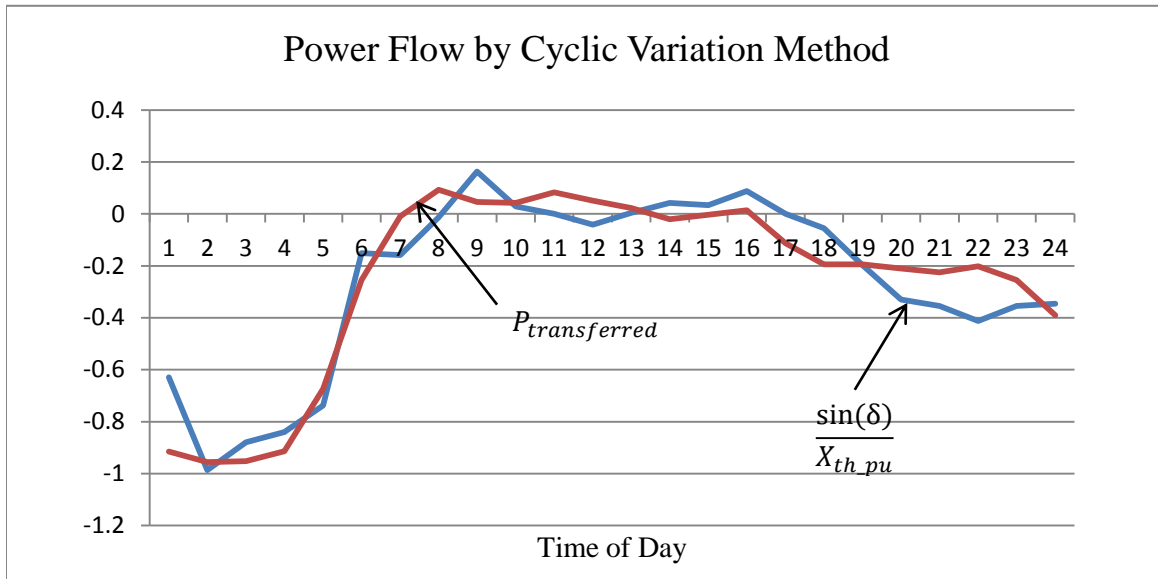


Figure 22:Feb25th-Power Flow by Cyclic Variation Method

Day	A	B	C	$X_{th\_pu}$	Error
25-Feb-2011	287.84	11.66	2842.962	0.041	0.012

Table 10:Feb25th-Results by Cyclic Variation Method

The values for the Thevenin equivalent reactance obtained by both methods are consistent with values obtained for the remaining days in February and March.

#### 4.5 4<sup>TH</sup> MARCH 2011

The synchrophasor data obtained is analyzed using both methods. The results are presented in the following sections.

#### 4.5.1 Damping Ratio Method

The power flow curves obtained show a good fit for all intervals of the day as seen in Figure 23 and the Thevenin equivalent obtained is consistent for results in the month of February and March. The power flow curve obtained is consistent with that obtained by using the Cyclic Variation Method.

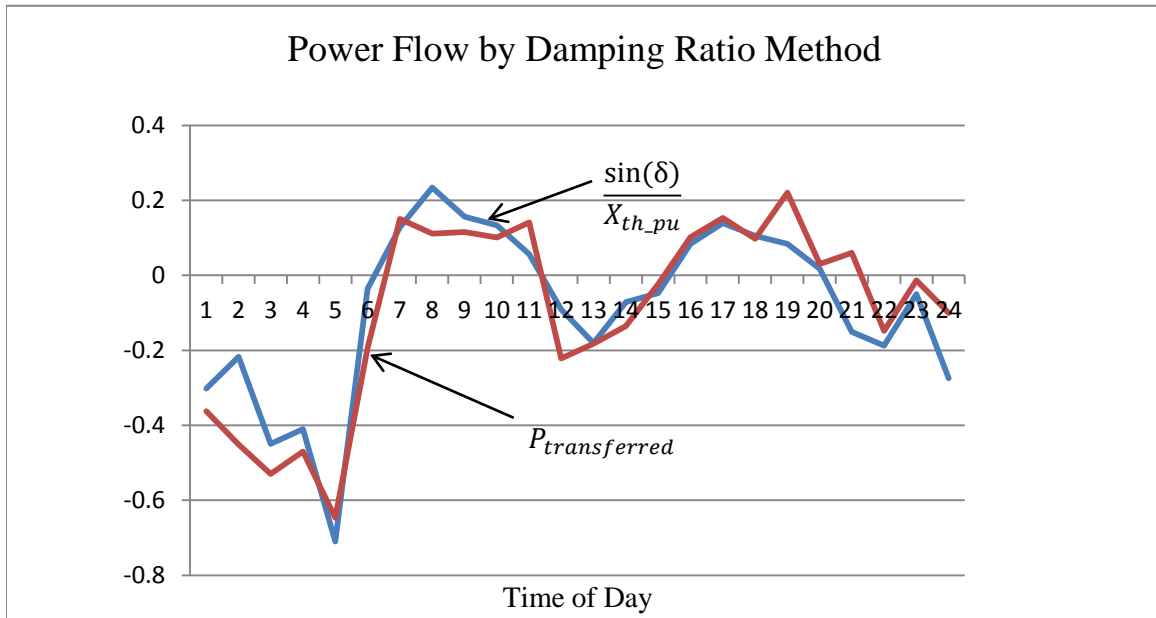


Figure 23:4thMar-Power Flow by Damping Ratio Method

Day	A	B	Xth_pu	Error
4-Mar-2011	1.2E4	989.41	0.04	0.03

Table 11:Mar4-Results by Damping Ratio Method

#### 4.5.2 Cyclic Variation Method

The Excel Solver gives us an estimate of the Thevenin Equivalent reactance which is consistent with that obtained by the Damping Ratio Method for the same day.

As expected, the power flow curves are also similar to those obtained by the Damping Ratio method. The results of the analysis are shown in Figure 24 and Table 12 below.

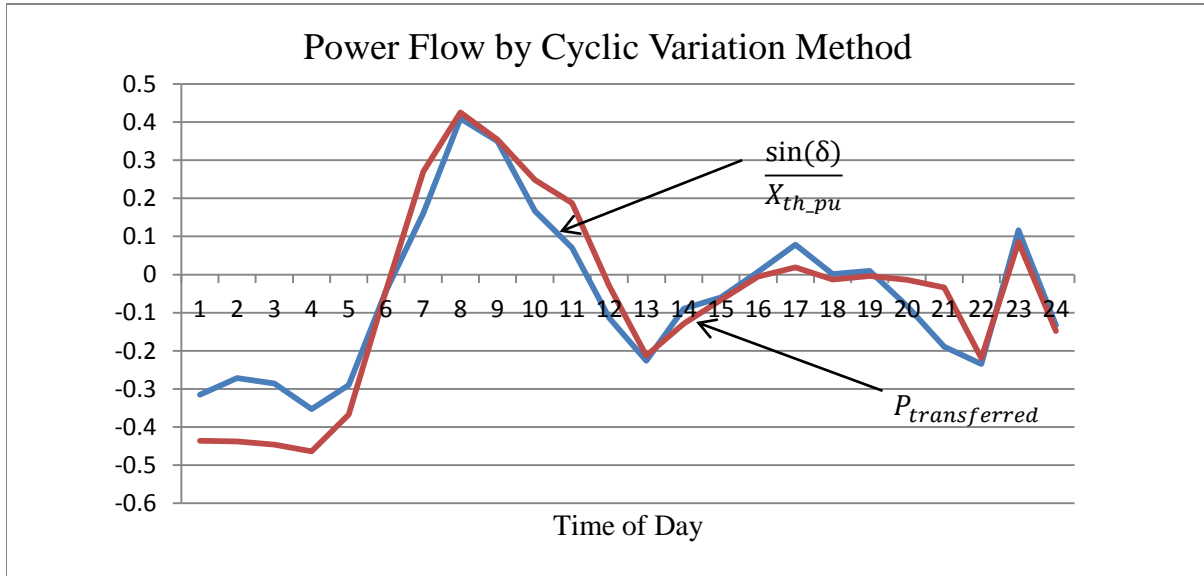


Figure 24:4th Mar-Power Flow by Cyclic Variation Method

Day	A	B	C	$X_{th\_pu}$	Error
4-Mar-2011	395.44	12.65	2351.55	0.043	0.0137

Table 12:4th March-Results by Cyclic Variation Method

#### 4.6 30<sup>TH</sup> MARCH 2011

The synchrophasor data obtained shows a spike in damping ratio at 03:00 CST due to an unknown grid event as shown in Fig.25 below. Such deviations in the damping ratio profile are generally expected to cause deviations in the power flow curves and calculated value for the Thevenin equivalent reactance. The effect of this particular grid event is studied in the following sections.

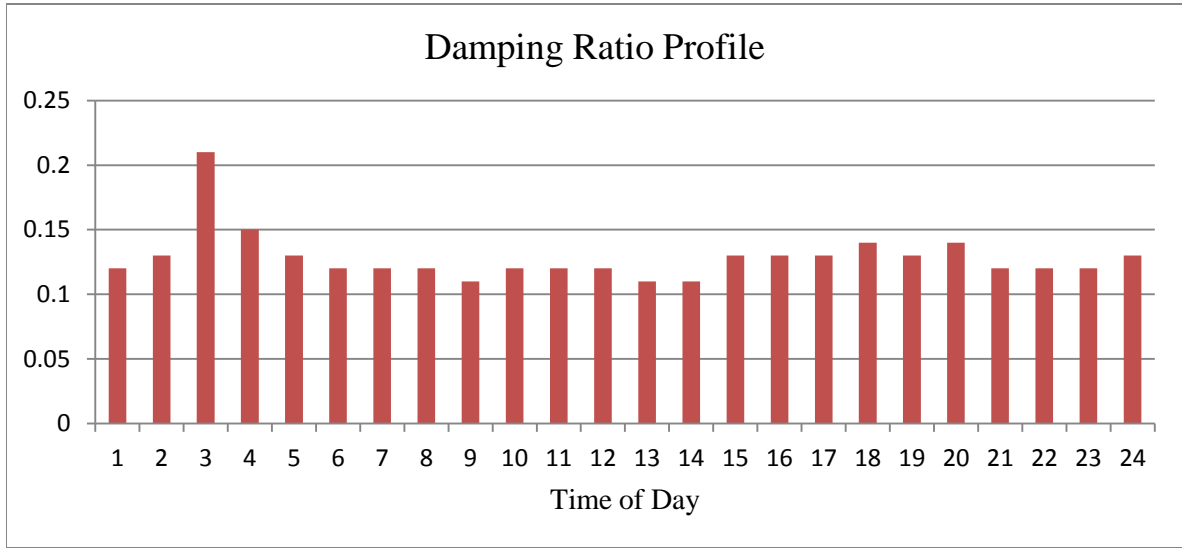


Figure 25:30th Mar-Damping Ratio Profile

#### 4.6.1 Damping Ratio Method

The power flow curves obtained by the Damping Ratio Method show a good curve fit at all intervals except for the duration of the grid event due to the generation  $P_{gen}$  being expressed as a function of the damping ratio  $\zeta$ .

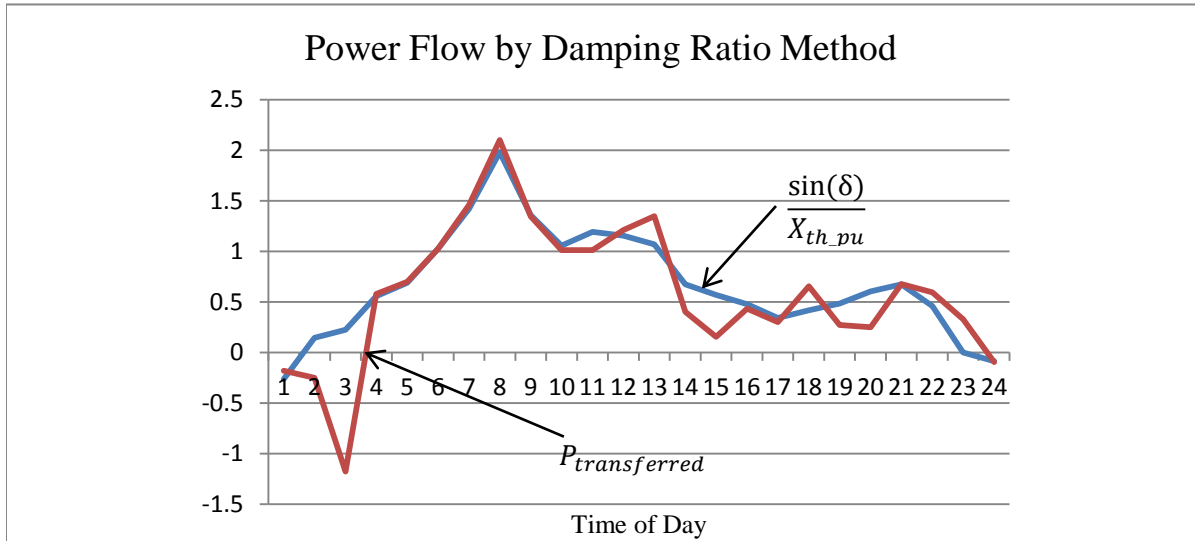


Figure 26:30th Mar-Power Flow by Damping Ratio Method

Day	A	B	$X_{th\_pu}$	Error
30-Mar-2011	1.01E4	1277.93	0.03	0.11

Table 13:30th Mar-Results by Damping Ratio Method

#### 4.6.2 Cyclic Variation Method

The power flow curves obtained do not show the effect of sudden spike in the damping ratio  $\zeta$ . The error obtained is smaller than by the Damping Ratio Method but the results for the Thevenin equivalent reactance are almost similar as shown in Table 14 below.

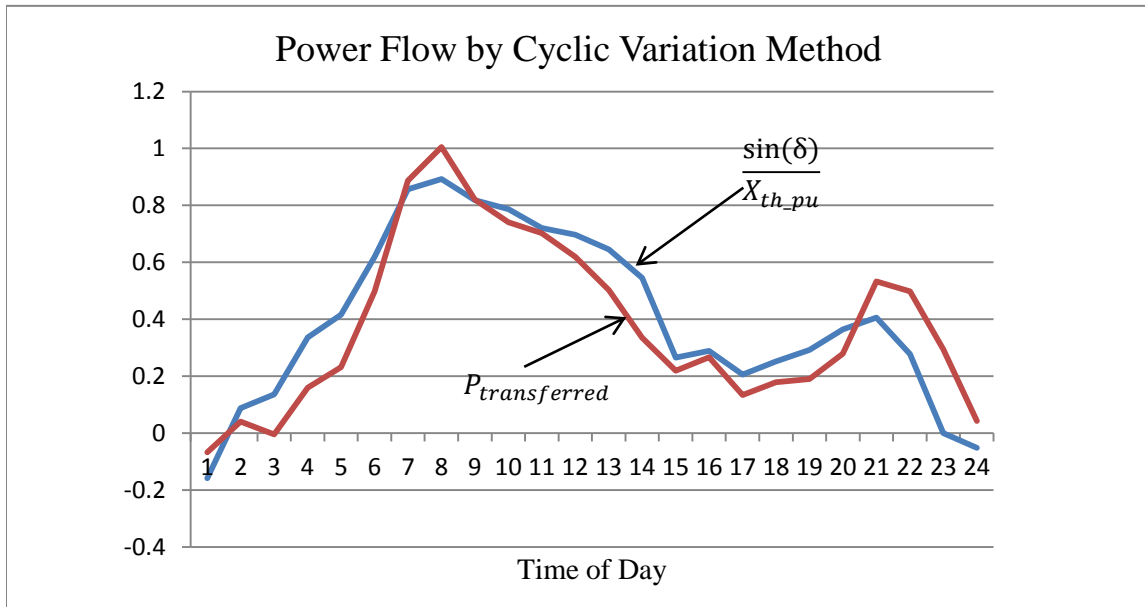


Figure 27:30th Mar-Power Flow by Cyclic Variation Method

Day	A	B	C	$X_{th\_pu}$	Error
30-Mar-2011	295.28	11	2382.65	0.04	0.01

**Table 14:30th Mar-Results by Cyclic Variation Method**

The grid event which causes a spike in the Damping Ratio affects the power flow curves obtained by using this method. However the values for the Thevenin equivalent reactance obtained by both methods are similar showing that the grid event does not affect the results obtained by the Excel Solver. However, another grid event on 8<sup>th</sup> April affects the value for the Thevenin Equivalent reactance as shown in a later section. With knowledge of the precise nature of grid events readily available, the effect of these events on the grid parameters can be analyzed and effective control strategies can be implemented.

#### **4.7 2<sup>ND</sup> APRIL 2011**

Unlike the previous day for which synchrophasor data is available i.e. 30<sup>th</sup> March 2011, the damping ratio profile for 2<sup>nd</sup> April does not show any anomalous data points. The two methods are implemented to determine the Thevenin equivalent reactance and the results are presented in the following sections.

##### **4.7.1 Damping Ratio Method**

The synchrophasor data is entered into an Excel Spreadsheet and the Excel solver is used to estimate the value of the Thevenin Equivalent reactance. As can be seen from Fig 28 and Table 15 below, we get a good curve fit between the two power flow curve estimates with a low value of error.

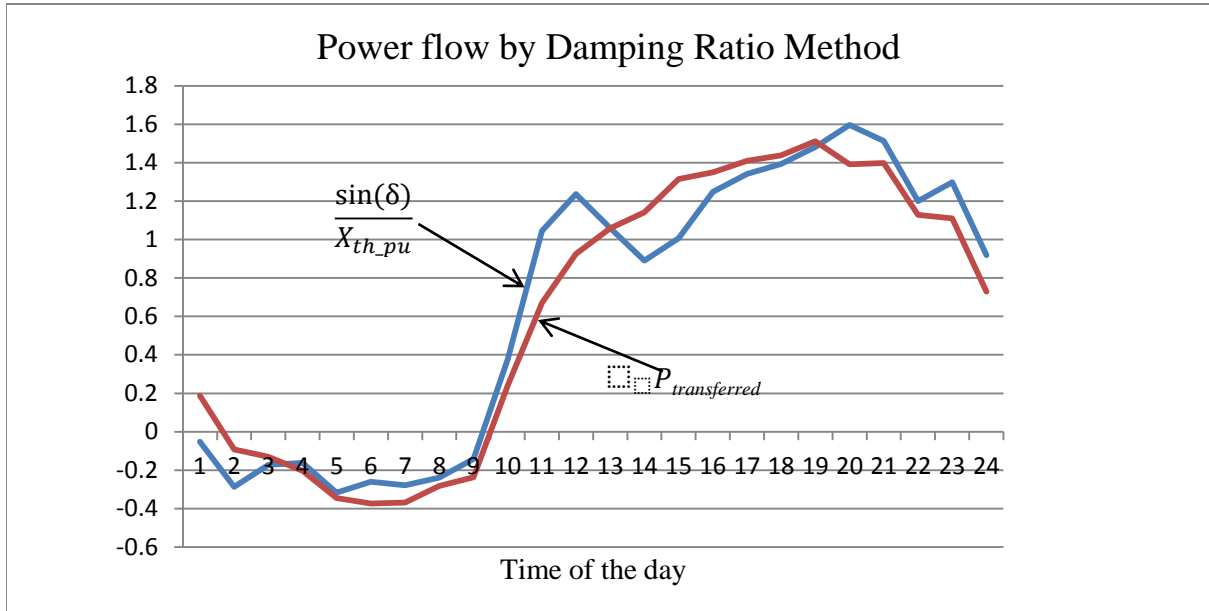


Figure 28:2nd Apr-Power Flow by Damping Ratio Method

Day	A	B	$X_{th\_pu}$	Error
2-Apr-11	1.2E4	2536.794	0.026	0.04

Table 15:2nd Apr-Results by Damping Ratio Method

#### 4.7.3 Cyclic Variation Method

The results of the analysis on synchrophasor data by The Cyclic Variation Method are presented below. As can be seen from Fig. 29 and Table 16 below, the values obtained for the Thevenin equivalent reactance are similar to those obtained by the Damping Ratio method. The power flow curves obtained by both methods are also similar.

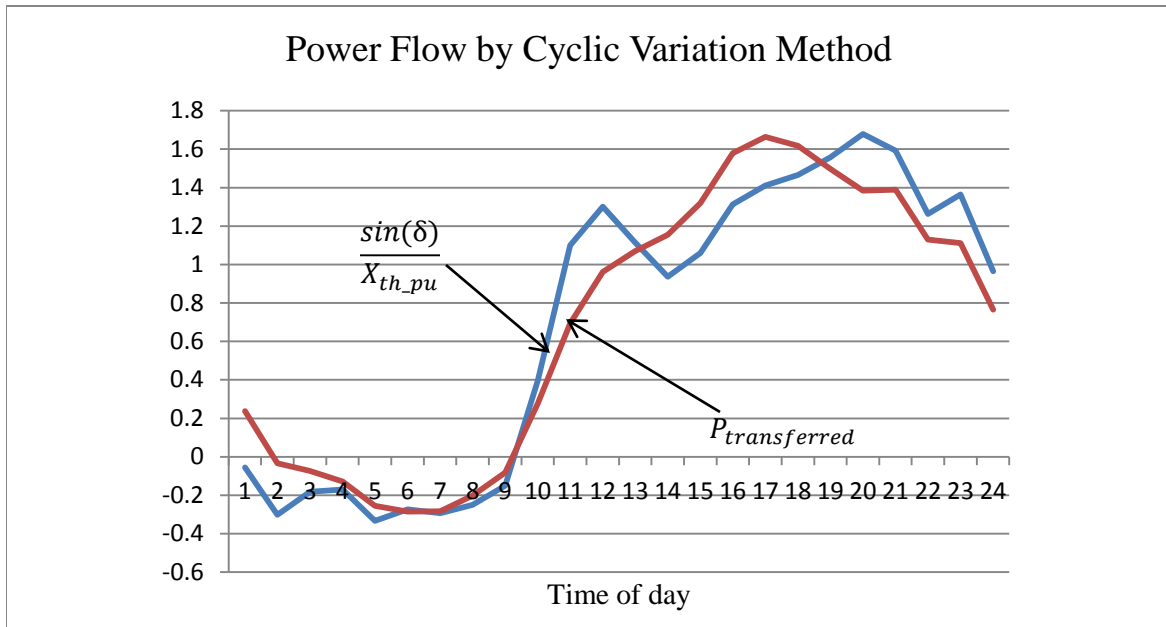


Figure 29:2nd Apr-Power Flow by Damping Ratio Method

Day	A	B	C	$X_{th\_pu}$	Error
2-Apr-2011	251.33	13.55	2677.1	0.0249	0.06

Table 16:2nd Apr-Results by Damping Ratio Method

We get similar values for Thevenin equivalent reactance from both methods as can be seen from Tables 15 and 16. The power flow curves obtained by both methods are also similar with low error. The value of  $X_{th\_pu}$  obtained by both methods, though similar is somewhat lower than those obtained on most days. With the synchrophasor data available to us at the moment, an explanation of this decrease in Thevenin Equivalent reactance is however not possible.



#### 4.8 3<sup>RD</sup> APRIL 2011

The synchrophasor data obtained for 3<sup>rd</sup> April is analyzed using both methods. The damping ratio and load profile are similar to those obtained on the previous day and we expect similar results for the Thevenin equivalent reactance.

##### 4.8.1 Damping Ratio Method

We get a good curve fit for all intervals of the day as shown in Figure 30 below. The Thevenin equivalent reactance obtained is close to the value obtained for 2<sup>nd</sup> April as predicted with a low value of error.

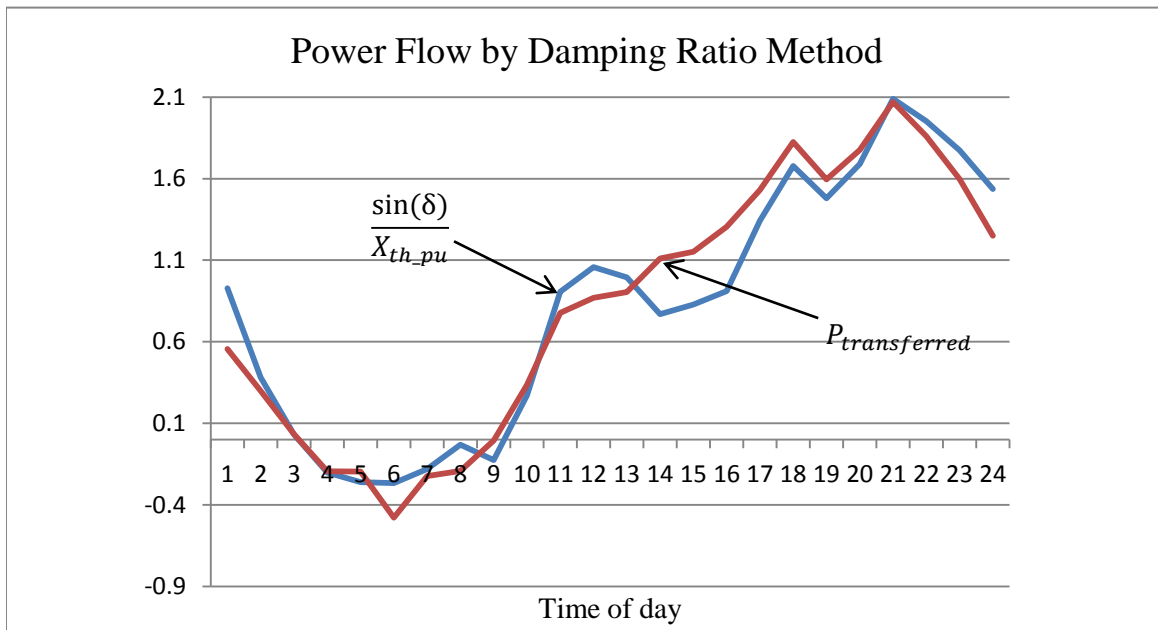


Figure 30:3rd April-Power Flow by Damping Ratio Method

Day	A	B	$X_{th\_pu}$	Error
3-Apr-2011	0.6E4	1594.65	0.022	0.034

Table 17:3rd April-Results by Damping Ratio Method

#### 4.8.2 Cyclic Variation Method

The results of the analysis on synchrophasor data by The Cyclic Variation Method are presented below. As can be seen from Figure 30 and Table 18 below, the values obtained for the Thevenin equivalent reactance are similar to those obtained by the Damping Ratio method. The power flow curves obtained by both methods are also similar.

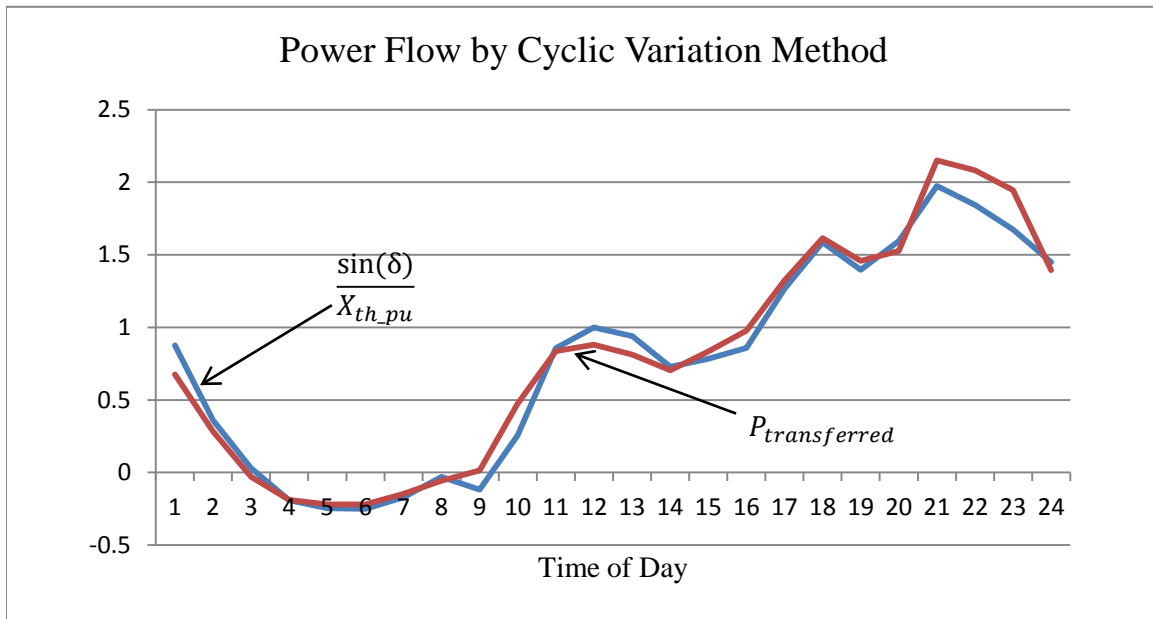


Figure 31:3rd April-Results by Cyclic Variation Method

Day	A	B	C	$X_{th\_pu}$	Error
3-Apr-2011	527.3	13.03	2951.83	0.021	0.003

Table 18:3rd April-Results by Cyclic Variation Method

As predicted, we get a similar result for the Thevenin equivalent reactance and power flow curves as obtained for April 2<sup>nd</sup> 2011. This strengthens the assumption about the strong correlation between the damping ratio ( $\zeta$ ) and power generation  $P_{gen}$ .

#### 4.9 8<sup>th</sup> APRIL 2011

Analysis of the synchrophasor data obtained on April 8<sup>th</sup> 2011 shows an anomalous data point for damping ratio at 14:00 CST. The profile for the grid damping ratio is shown in Figure 32 below

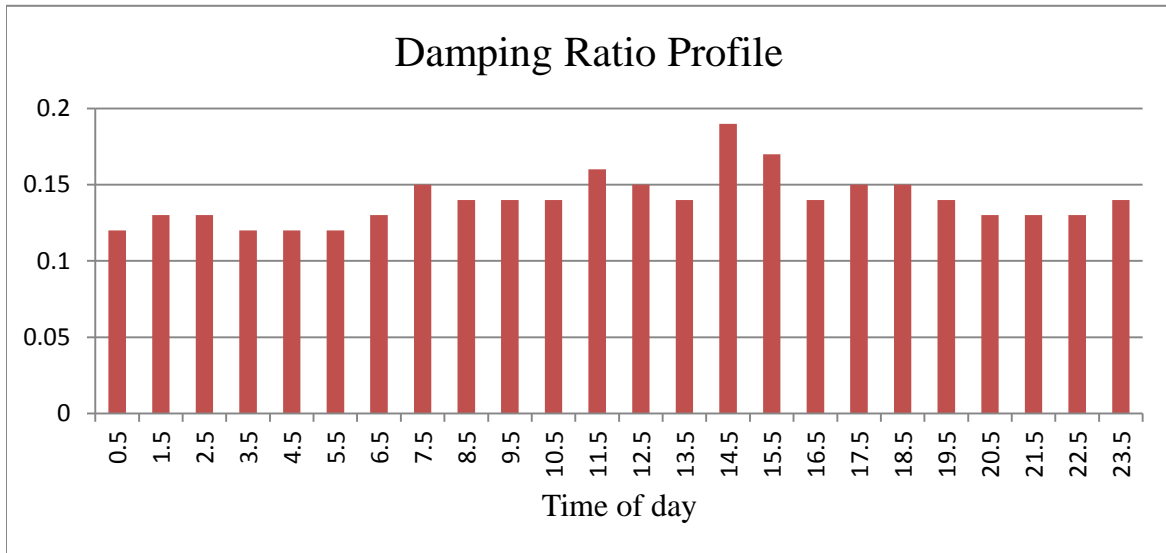
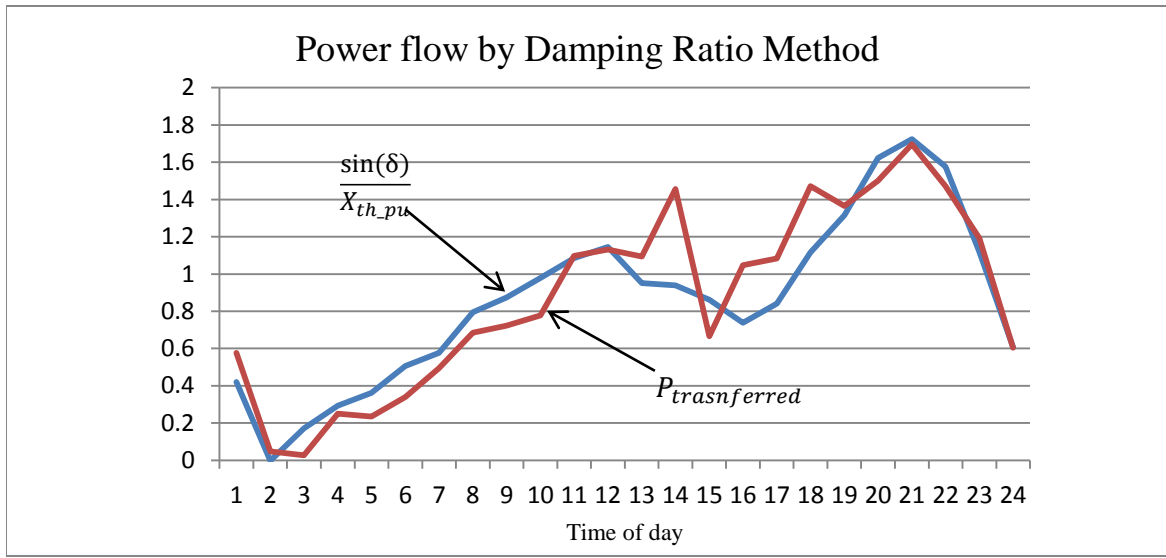


Figure 32: 8th Apr-Damping Ratio Profile

This sudden spike in the damping ratio is expected to cause slight errors in the measurement of  $X_{th\_pu}$  and deviation from a good curve fit for the two power flow estimates using the Damping Ratio method. The results for the analysis are presented below

##### 4.9.1 Damping Ratio Method

As expected, the anomaly in the damping ratio data due to an unknown grid event causes deviation in the curve fit as shown below. As only 24 data points are available for each each day, eliminating the anomalous data point does not result in a better curve fit.



**Figure 33:8th Apr-Power Flow by Damping Ratio Method**

Day	A	B	$X_{th\_pu}$	Error
8-Apr-2011	1.76E4	404.68	0.023	0.034

**Table 19:8th Apr-Results by Damping Ratio Method**

As can be seen from the power flow curve in Figure 33, a sudden spike occurs at 14:00 CST and causes a poor curve fit at this interval. A good curve fit is however obtained at all other intervals for this particular day.

#### 4.9.2 Cyclic Variation Method

As the Cyclic Variation in Generation method is independent of damping ratio, it is unaffected by the anomaly in Damping Ratio data. From Figure 34 below, it can be seen that a good curve fit is obtained for all intervals of the day.

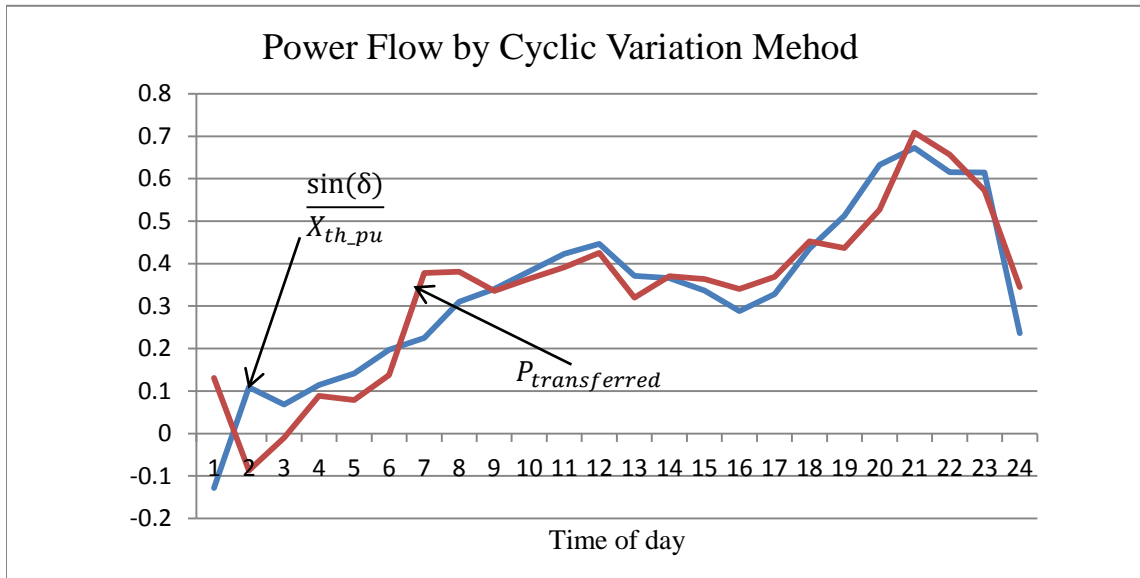


**Figure 34:8th Apr-Power Flow by Cyclic Variation Method**

Day	A	B	C	$X_{th\_pu}$	Error
8-Apr-2011	721.77	13.42	3391.77	0.049	0.007

**Table 20:8th Apr-Results by Cyclic Variation Method**

As expected the waveforms for the power flow obtained by both methods are almost identical for most intervals of the day. The difference in waveforms is caused by the grid event at 14:00 CST which causes a spike in the damping ratio of the grid to 0.19. This increase in damping ratio affects the solution of the power flow equation in the Damping Ratio method due to the generation  $P_{gen}$  being expressed as a function of the damping ratio but has no effect on the Cyclic Variation in Generation method. The event is also responsible for the difference in values of the Thevenin equivalent reactance obtained by both methods.

#### 4.10 11<sup>TH</sup> APRIL 2011

The synchrophasor data obtained is analyzed using both methods to obtain the Thevenin equivalent reactance. The results of the analysis are presented below.

##### 4.10.1 Damping Ratio Method

As can be seen from Figure 35 below, there is a good curve fit between the two power flow estimates for the entire day. The error is also greatly reduced from the results obtained on April 8<sup>th</sup> 2011.

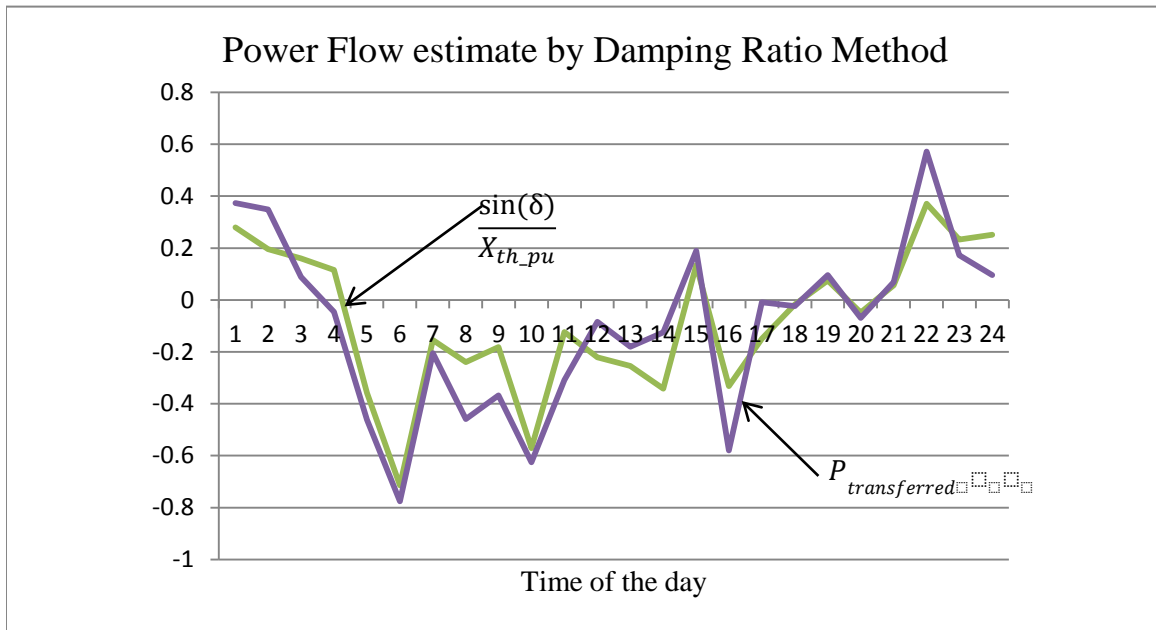


Figure 35:10 Apr-Power Flow by Damping Ratio Method

Day	A	B	$X_{th\_pu}$	Error
11-Apr-2011	1.34E4	1299.79	0.05	0.017

Table 21:11 Apr-Results by Damping Ratio Method

#### 4.10.2 Cyclic Variation Method

The Cyclic Variation in Generation method also provides a good fit between the two power flow estimates for the entire duration of the day as shown in Figure 36. We obtain a realistic estimate for the Thevenin Equivalent reactance with a very low error.

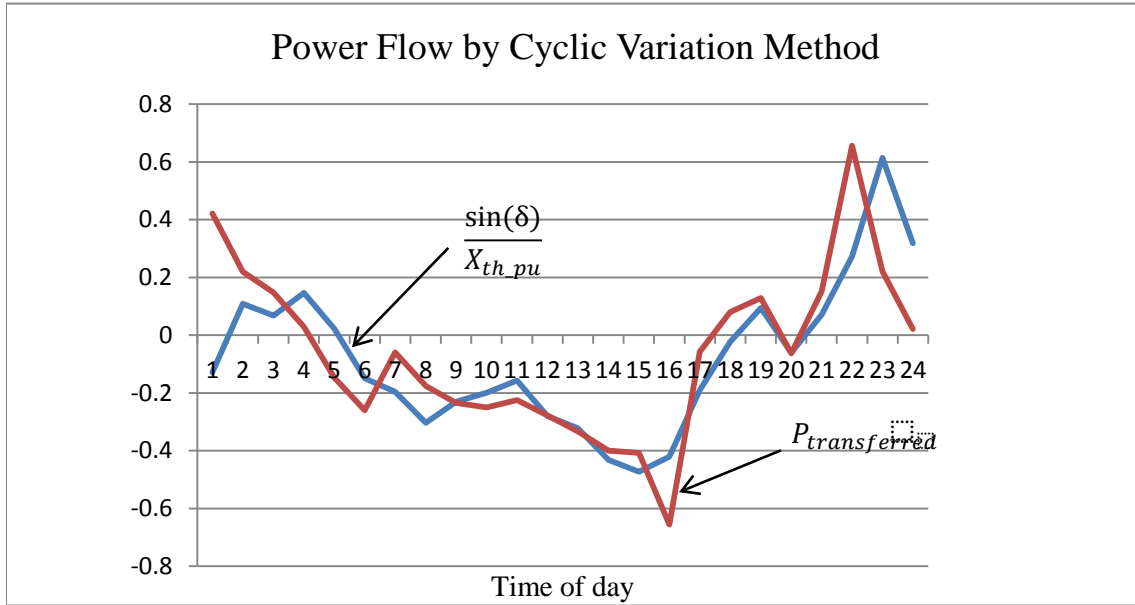


Figure 36:11th Apr-Power Flow by Cyclic Variation Method

Day	A	B	C	$X_{th\_pu}$	Error
11-April-2011	611.25	14.16	3310.02	0.044	0.037

Table 22:11th Apr-Results by Cyclic Variation Method

The curves obtained are similar to those obtained by the Damping Ratio Method. The values of  $X_{th\_pu}$  obtained by both methods are quite close to each other with a very small resultant error

## **CHAPTER 5**

### **CONCLUSION**

Computing the Thevenin Equivalent reactance is an important step in stability and contingency analyses for more secure and stable power systems. In this thesis we propose two separate methods which utilize known synchrophasor data to estimate the power flow between The University of Texas at Austin and The University of Texas at PanAm and to determine the Thevenin equivalent reactance. The methods differ from each other in the way the generation is represented as a function of known phasor data. The results obtained by both methods are in agreement with each other and it is seen that the Thevenin equivalent reactance lies within a range of 0.027 to 0.041 p.u on a 100 MVA base. The variation in the results for the equivalent reactance can be explained by grid events which cause anomalies in the damping ratio data obtained on a particular day and deviations from the expected load profile on certain days. To validate the Thevenin Equivalent Reactance we apply the universal Cyclic Variation in Load Method on synchrophasor data for West Texas as shown in [http://users.ece.utexas.edu/~grady/34\\_EE394J\\_Spring11\\_Thevenin\\_Example\\_March\\_1\\_2011.ppt](http://users.ece.utexas.edu/~grady/34_EE394J_Spring11_Thevenin_Example_March_1_2011.ppt). The results for the Thevenin Equivalent Reactance correspond to values obtained in existing literature on the subject. [5]

The results obtained for the Thevenin equivalent reactance lie within a realistic range but accuracy is compromised as only 24 data points are available for a particular day as of now. The availability of load information on a minute by minute basis can help improve accuracy of obtained results and result in a better curve fit between the two



estimates for the power flow by eliminating intervals in which anomalous data is present. Daily Grid Operation reports if available can be used to make invaluable observations about the effects of grid events on the grid damping ratio, damping frequency and power flow.

## REFERENCES

- [1] Wadhwa C.L; Electrical Power System, New Age Publishers, Delhi 2004
- [2] D'Antona, G.; Monti, A.; Ponci, F., "A Decentralized State Estimator for Non-Linear Power Systems," Systems Conference, 2007 1st Annual IEEE, vol., no., pp.1-6, 9-13 April 2007
- [3] "IEEE Standard for Synchrophasors for Power Systems", IEEE Std C37.118-2005
- [4] Grady, W.M.; Costello, D., "Implementation and application of an independent Texas synchrophasor network," Protective Relay Engineers, 2010 63rd Annual Conference for, vol., no., pp.1-12, March 29 2010-April 1 2010
- [5] P.A. Kowley, "Synchrophasor based method for computing the Thevenin equivalent impedance seen by a concentrated wind farm region", pp. 1-56, Engineering 2010